NEUROPROTECTIVE EFFECT OF INTRAOCULAR BDNF AND OPTOGENETIC STIMULATION OF VISUAL CORTEX ON RETINAL GANGLION CELL SURVIVAL AND FUNCTION IN THE RAT FOLLOWING OPTIC NERVE INJURY

By

Fatma Madi

A THESIS

Submitted to
Michigan State University
in partial fulfillment of the requirements
for the degree of

Physiology - Master of Science

2018

ABSTRACT

NEUROPROTECTIVE EFFECT OF INTRAOCULAR BDNF AND OPTOGENETIC STIMULATION OF VISUAL CORTEX ON RETINAL GANGLION CELL SURVIVAL AND FUNCTION IN THE RAT FOLLOWING OPTIC NERVE INJURY

By

Fatma Madi

Glaucoma is an optic neuropathy characterized by a progressive degeneration of retinal ganglion cells (RGCs) and their axons. The RGC loss is thought to result, in part, from a decrease in target-derived trophic material. This is supported by studies showing that direct injections of trophic factors into the injured eye are beneficial. Unfortunately, they do not provide long-term neuroprotection. Previous work in our lab has indicated that treatment of the entire central visual pathway (CVP) is more beneficial long-term vs treatment of the eye alone. While those studies involved direct application of trophic factor to the eye and visual cortex, the present studies apply an optogenetic approach to induce enhanced endogenous levels of CVP trophic factors.

Measurement of RGC survival following optic nerve injury and treatment of the eye combined with optogenetic stimulation of visual cortex showed significant improvement compared to no treatment or treatment of the eye alone, supporting our theory that future development of glaucoma treatment strategies must involve treatment of the entire central visual pathway, and not just treatment of the eye, as is the current convention.

ACKNOWLEDGEMENTS

I would like to acknowledge and thank all the sacrificed animals used in this study. I would like to thank my mentor, Dr. Arthur Weber for being a great advisor and teacher, and for his patience throughout this project. I would like to thank him for teaching me the necessary laboratory skills concerning the handling of research animals, surgical procedures, tissue preparation, retinal dissection, and IHC techniques that were essential to my project and to progress in my scientific future. I would like to thank my committee members, Dr. Susanne Mohr and Dr. Julia Busik, who have always been supportive and kind, and for their input and advice towards my work. My sincere thanks to our collaborators, Dr. Wen Li and the members of her lab. I would thank Dr. Marianna Bacellar for all her assistance and patience with the rat electroretinography procedures. I too would like to acknowledge all of the MSU core facilities including: Histopathology Lab, Animal Care Facility, Veterinary Medical Center, and Confocal Laser Scanning Microscopy. I would like to acknowledge the National Science Foundation, the Libyan-North American Scholarship Program, Libyan Ministry of Higher Education and Scientific Research, The Biological Sciences Program, Departments of Physiology and Department of Electrical and Computer Engineering at Michigan State University.

I greatly appreciate Dr. Susanne Mohr for her great support and encouragement not only as a graduate program director but also as a friend. I would like thank Amy Porter and Kathy Joseph for their friendship and kindness. Finally, I would like to thank my family and all of my friends for support, inspiration and forgiveness.

TABLE OF CONTENTS

LIST OF FIGURES

KEY TO ABBREVIATIONS

AAV …… Adeno-associated viral

AC …… Area centralis

ANOVA …….. Analysis of variance

ARVO …….. Association for Research in Vision and Ophthalmology

ATP …….. Adenosine triphosphate

Bcl-2 …….. B-cell lymphoma 2

Bcl-xl …….. B-cell lymphoma-extra large

BDNF …….. Brain-Derived Neurotrophic Factor

cAMP …… Adenosine 3',5'-cyclic monophosphate

ChR …… Channel rhodopsin receptor

CNTF …….. Ciliary neurotrophic factor

CREB …….. cAMP response element-binding protein

Ctx …….. Cortex

DAB …… 3,3'-diaminobenzidine

DAPI …….. 4’,6-diamino-2-phenylindole

DNA …… Deoxyribonucleic acid

DT …… Dual treatment

ER …… Endoplasmic reticulum

ERG …… Electroretinography

FAS …….. First apoptosis signal receptor

G-protein ……. Guanine nucleotide binding protein

LC …….. Lamina cribrosa

LED …… Light emitting diode

MAPK/ERK …….. Mitogen-Activated Protein Kinases/Extracellular Signal-Regulated Kinase

NGF …….. Nerve growth factor

NO …….. Nitric oxide

nSTR …….. Negative scotopic threshold response

NT …….. Neurotrophins

NTF …… Neurotrophic factor

p75NT ……. p75 Neurotrophin Receptor

PBS …… Phosphate buffer saline

PI3K/Akt …… Phosphatidylinositol-3-Kinase and Protein Kinase B

POAG …….. Primary open-angle glaucoma

pSTR …….. Positive scotopic threshold response

RBPMS …… RNA-binding protein with multiple splicing

RGC …….. Retinal ganglion cell

ROS …….. Reactive Oxygen Species

STR …… Scotopic threshold response

TM …….. Trabecular meshwork

TNF-α ……. Tumor necrosis factor alpha

Trk …….. Tyrosine receptor kinase

INTRODUCTION

Glaucoma is the second leading cause of irreversible blindness globally. It affects more than 70 million people worldwide, of which 10% are bilaterally blind. In the United States, approximately 2 million people have been diagnosed with glaucoma, resulting in 120,000 cases of blindness, and a cost of more than $1.5 billion.[1-3] The Glaucomas are a multifactorial group of optic neuropathies characterized by a progressive degeneration of retinal ganglion cells (RGCs) and their axons, structural changes in the appearance of the optic nerve head, and characteristic visual field defects.[4-6] Of the more than 30 types of glaucoma, the two most common are open and closed angle. Both can be subdivided into primary (unknown etiology), or secondary (known etiology – e.g. inflammation, vasculopathy, trauma, tumor, pigmentation dispersion, etc.). [5-6] Typically, the aqueous humor that bathes the front of the eye flows from the posterior chamber to the anterior chamber and is drained into the venous system via its primary route though the trabecular meshwork near the margin of the cornea (Fig. 1A). In primary open angle glaucoma (POAG) a yet to be identified mechanism causes an increase in the outflow resistance of aqueous humor, resulting in a buildup of fluid and an increase in intraocular pressure (IOP) (Fig. 1-B). [7-9] By contrast, in closed angle glaucoma the iris physically obstructs the outflow pathway (Fig. 1-C). Risk factors of glaucoma are many, including increased IOP, age, male sex, family history, and race. African American and Hispanic populations are at a higher risk to develop glaucoma and blindness than Caucasians, while closed angle glaucoma is more prevalent among Asian people. Moreover, there also are ocular risk factors, such as high myopia. Hypertension and diabetes also

have been indicated as potentially being involved in an increased risk of developing glaucoma. [2, 5, 7-10, 24] Although, IOP continues to be a primary risk factor, it no longer is required for a diagnosis

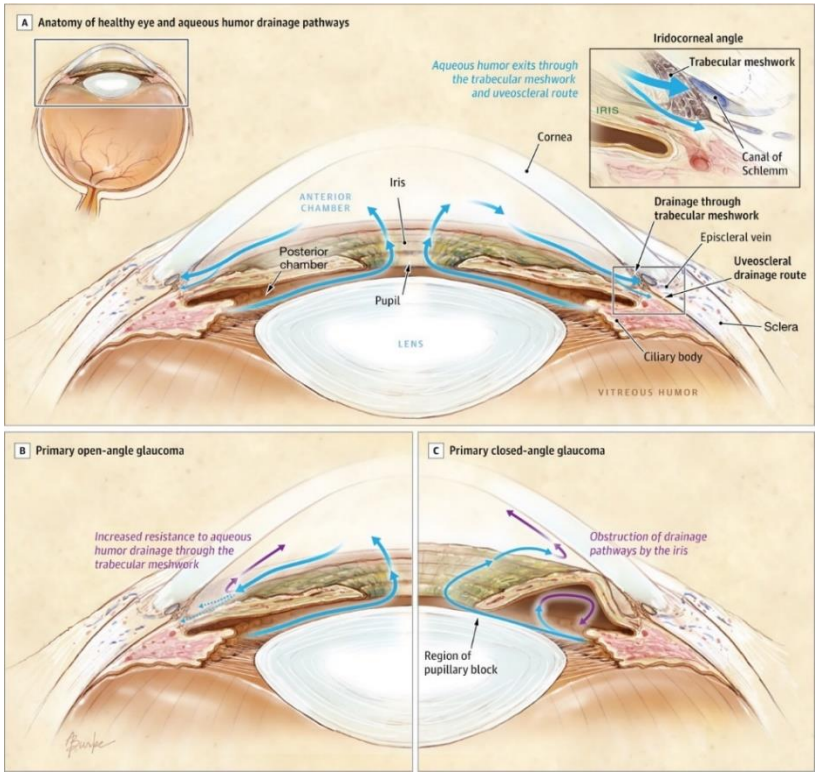

Figure 1: Aqueous humor circulation: A) Normal Eye: Aqueous humor is excreted by the ciliary muscle into the posterior chamber where it flows between the iris and lens up through the pupil to enter the anterior chamber, and then is resorbed into the venous system by the trabecular meshwork route or uveoscleral, route. Zoomed view shows aqueous humor drainage by the trabecular meshwork into a channel called Schlemm's canal, which then empties into the episcleral vessels, along with that from the uveoscleral pathway. B) Open angle glaucoma: increased the resistance of aqueous humor drainage through the trabecular meshwork (TM) near the margin of the cornea causes an elevation of IOP. C) Closed angle glaucoma: The iris physically obstructs the major outflow pathway for the aqueous humor leading to a buildup of fluid and an increase of IOP. Weinreb et al (2014). [60]

of glaucoma. [7, 9] Studies have shown that roughly half of patients diagnosed with POAG based on examination of their eyes have IOPs within the statistically 'normal' range of 16-20 mm Hg. [4, 7, 8] By contrast, other patients have higher than 'normal' levels of IOP (> 21 mmHg), yet they don't

develop glaucoma. [9] The former group are considered to have 'normotensive' glaucoma, while the later are referred to as 'ocular hypertensive'. While studies have shown that a 20% reduction in IOP, even in glaucoma patients with 'normal' IOP, effectively reduces the progression of RGC loss, it is important to note that this treatment strategy is effective in only about 50% of glaucoma patients. [5]

Besides elevated IOP, disc 'cupping' and visual field loss are the two other clinically characteristic features of glaucoma. Cupping, or deepening, of the optic disc at the back of the eye occurs as a result of the loss of retinal ganglion cell axons as they exit the eye and form the optic nerve by which visual information is transferred to higher centers of the brain (Fig. 2-A) [5, 9, 11]. Visual field deficits also are the result of retinal ganglion cell degeneration. Interestingly, patients may experience up to a 40% loss of retinal ganglion cells before visual deficits are detected [5]. While cells in all regions of the retina are affected, in most cases the visual field loss starts with the patient's peripheral vision and progresses centrally, ultimately resulting in tubular vision, followed by blindness (Fig. 2-B).[9]

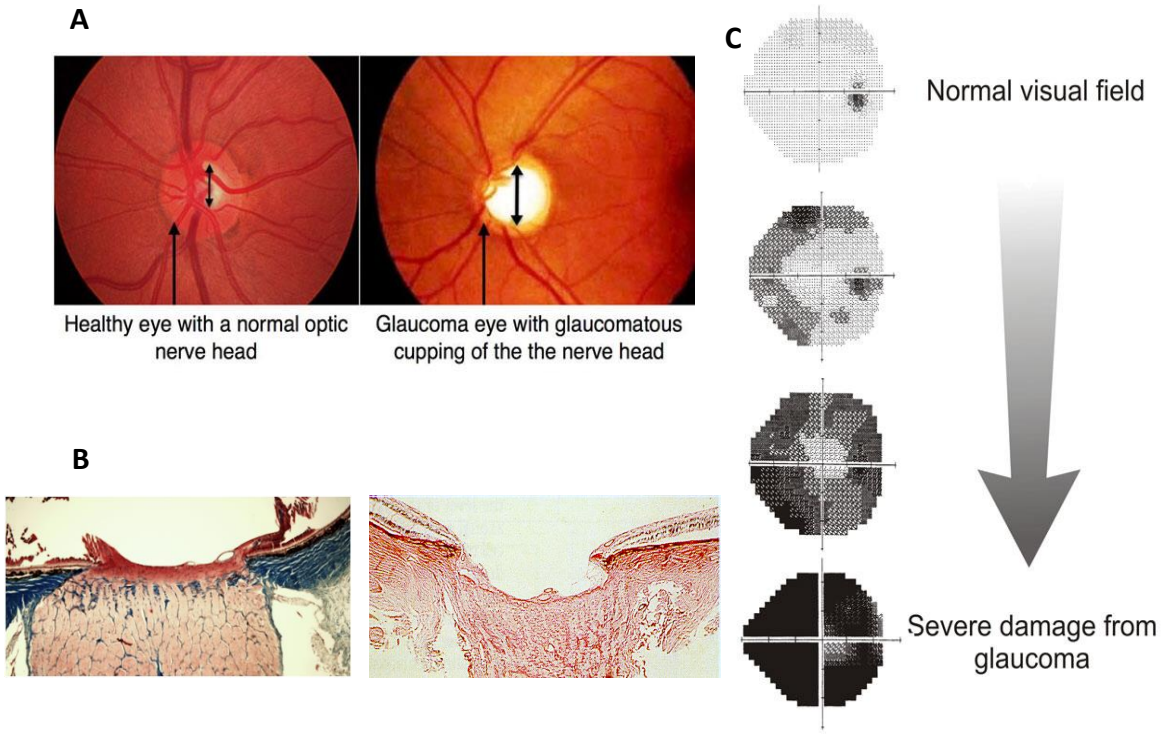

Figure 2: Glaucoma characteristic features: A) Optic disc appearance by funduscopy: Left: Normal Eye with normal optic cup/disc ratio. Right: Glaucomatous eye showing increased cup/disc ratio due to the loss of retinal ganglion cell axons as they exit the eye and increased pallor due to disruption of the vasculature. Retrieved from http://www.ranelle.com/wp-content/uploads/2016/08/glaucoma-cupping-of-nerve-head-1024x932.jpg B) Micrographs of cross-sections of the optic nerve head of a normal eye (left) compared to a glaucomatous eye (right) showing optic nerve head cupping and axonal loss. From Weber et al. (1998). [64] C) Progressive vision loss in glaucoma patient: the visual field loss starts with the patient's peripheral vision and progresses centrally. Weinreb et al (2014). [60]

ANATOMY OF THE EYE

The main structures of the eye are the anterior, posterior, and vitreal chambers, the tissue layers (sclera, choroid, retina), and the refractive elements, which include the cornea, lens, and ciliary muscle. [12, 13] The chambers contain the important fluids of the eye. The vitreal chamber occupies the posterior region of the eye and is filled with the jelly-like vitreous humor, which helps to preserve the shape of the eye. The smaller anterior and posterior chambers, located between the cornea and iris and the iris and lens, respectively, are filled with aqueous humor (Figs. 1-A and 3-A).

The aqueous humor functions to supply the avascular lens and cornea with oxygen and nutrients, and remove metabolites. It also is responsible for maintaining the IOP of the eye. Aqueous humor is released by the vasculature of the ciliary muscle into the posterior chamber where it flows between the iris and lens up through the pupil to enter the anterior chamber. The aqueous humor circulates within the anterior chamber, and then is resorbed into the venous system by two main routes. The conventional route is through the trabecular meshwork, a sponge-like cellular tissue that encircles the eye at the margin of the iris and cornea. The unconventional, or uveoscleral, route is less well defined and includes seepage around and between the various tissues of the front of the eye, such as the iris, sclera, choroidal vessels etc. Aqueous humor that exits the eye via the trabecular meshwork drains into a channel called Schlemm's canal, which then empties into the episcleral vessels, along with that from the uveoscleral pathway (Fig. 1-A). [12, 13]

Structurally, the eye is composed of three layers; the sclera, along with the cornea, form the outer layer, the vascular choroid forms the middle layer, and the neural retina covers the posterior two thirds of the interior surface of the globe. The retina consists of several different cell types that are arranged in layers. From outside to inside, these include the: 1) pigment epithelium, 2) photoreceptor outer segment layer, 3) outer nuclear layer (photoreceptor cell bodies), 4) inner nuclear layer (bipolar, amacrine, and horizontal cell bodies), and the 5) ganglion cell layer on the inner surface of the retina. The region between the outer and inner nuclear layer, where they interact with each other, is referred to as the outer plexiform layer. Similarly, the region of synapses between the neurons of the inner nuclear layer and ganglion cell layer is referred to as the inner plexiform layer (Fig. 3-B). [12-15] There are more than twenty different classes of retinal ganglion cells, but the two primary ones in primates are the midget cells, which represent 80% of the retinal ganglion cells, project their axons to the parvocellular layers of the visual thalamus, and are considered to have a primary role in spatial vision, and the parasol cells, which represent about 5% of the ganglion cells in the retina, project their axons to the magnocellular layers of the visual thalamus , and are thought to be concerned primarily with the analysis of temporal visual processing. [12]

The ganglion cells represent the output neurons of the retina, and it is their axons that exit from the eye at the optic disc and form the optic nerve. As the bundles of axons exit they pass through the lamina cribrosa (LC), a collagenous meshwork of connective tissue beams and optic nerve head astrocytes (Fig. 4). It is generally agreed that the LC is the site of initial neuronal degeneration in glaucoma, as discussed below. [11]

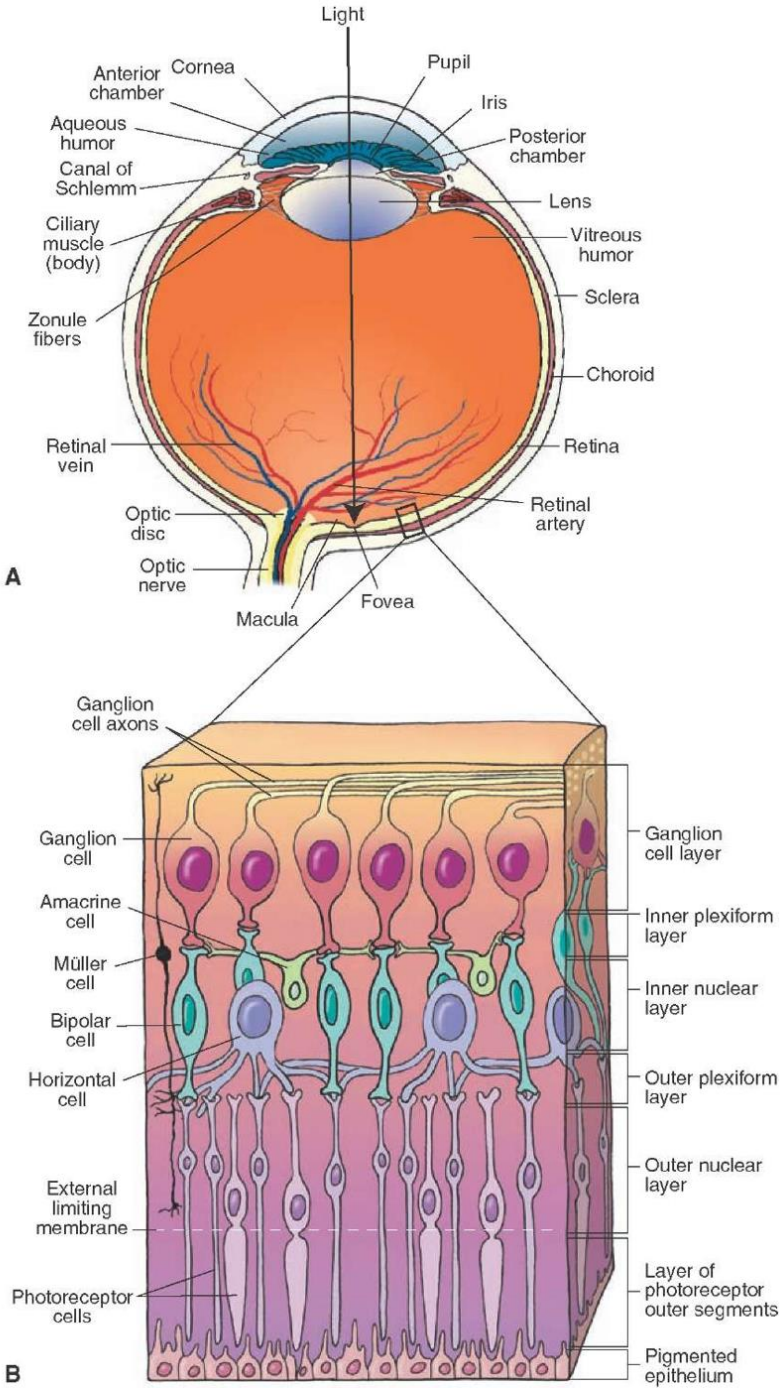

Figure 3: Anatomy of the eye: A) Main structures of eye. B) Detailed structure of retina shows its different layers and cells. Retrieved from http://what-when-how.com/neuroscience/visual-system-sensory-system-part-1/

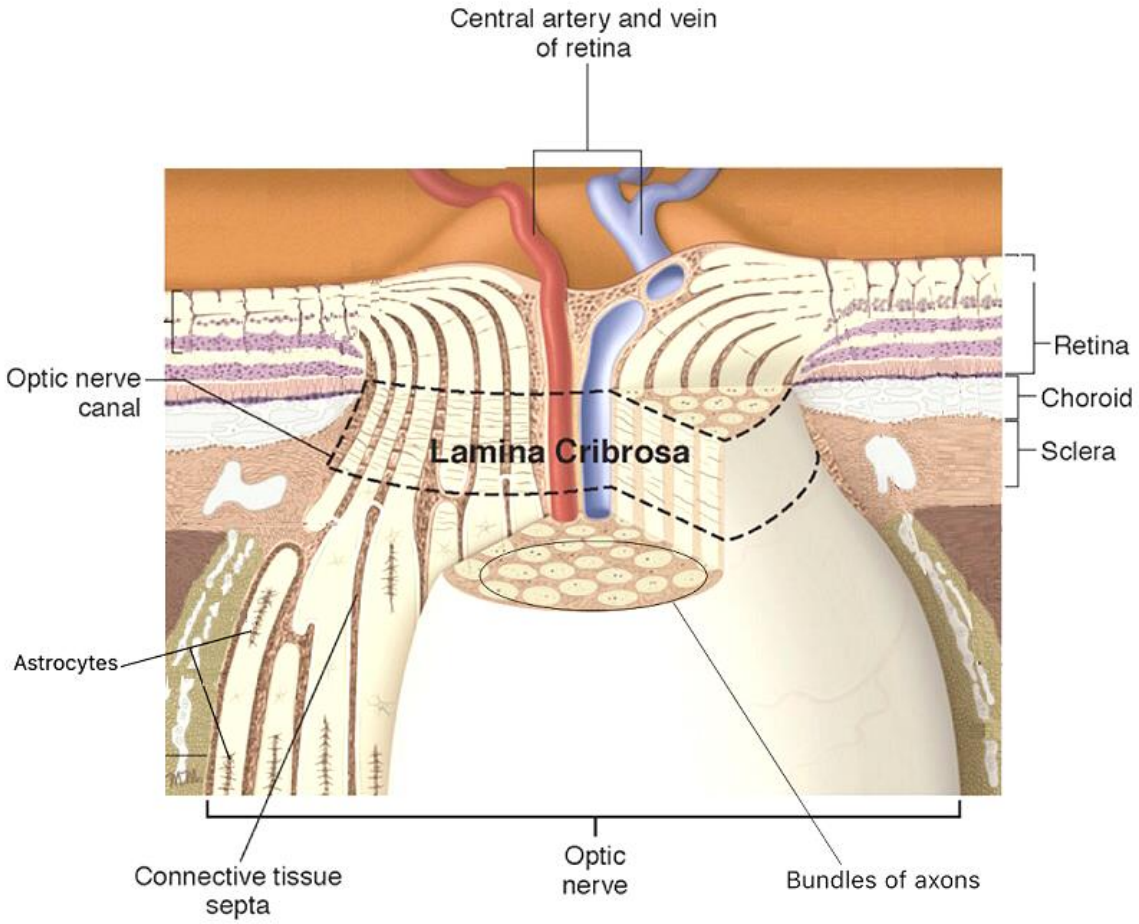

Figure 4: Lamina cribrosa: The lamina cribrosa (LC) is composed of collagenous meshwork of connective tissue beams, astrocytes and bundles of retinal ganglion cell axons that exit from the eye at the optic disc to form the optic nerve. Modified https://entokey.com/cranial-nerves-central-and-peripheral-connections

UNDERLYING MECHANISMS OF GLAUCOMATOUS NEUROPATHY

Impaired Axonal Transport of Supportive Materials

According to the mechanical theory, stress on the connective tissues of the lamina cribrosa due to elevated IOP results in compression of the nerve fiber bundles and disrupts both the retrograde (brain to retina) and anterograde (retina to brain) axonal transport of critical materials, particularly neurotrophic factors (Fig. 5). [5] Evidence in favor of this theory comes from studies that have shown a decrease in both retro- and anterograde axonal transport in animal models of experimental glaucoma. That the loss of transport of neurotrophic factors is involved is suggested by the fact that exogenous application of trophic materials to the eye is neuroprotective in these animals. [9, 11, 16-20]

However, a criticism of this theory is that it neither explains the variations in development of glaucoma by age, gender, or race in conjunction with IOP levels, nor patients with normotensive glaucoma. However, it has been suggested that these variations might be related to variations in the biomechanical properties of the lamina cribrosa tissues across different individuals. [5]

Vascular Dysregulation and Oxidative Stress

The ischemic theory suggests that perfusion insufficiency due to increased resistance to blood flow in fine capillaries caudal to the lamina cribrosa leads to the degeneration of retinal ganglion axons, and thus the ganglion cells themselves, whether or not IOP is elevated. [5, 9, 10, 25] Evidence for the ischemic theory includes a reduction of ocular blood flow in glaucoma patients, an

increased incidence of glaucoma in patients with systemic vascular disease, and increased levels of endothelin1, a vasoconstrictor, in the aqueous humor of glaucoma patients.[4, 5, 9, 22-24]

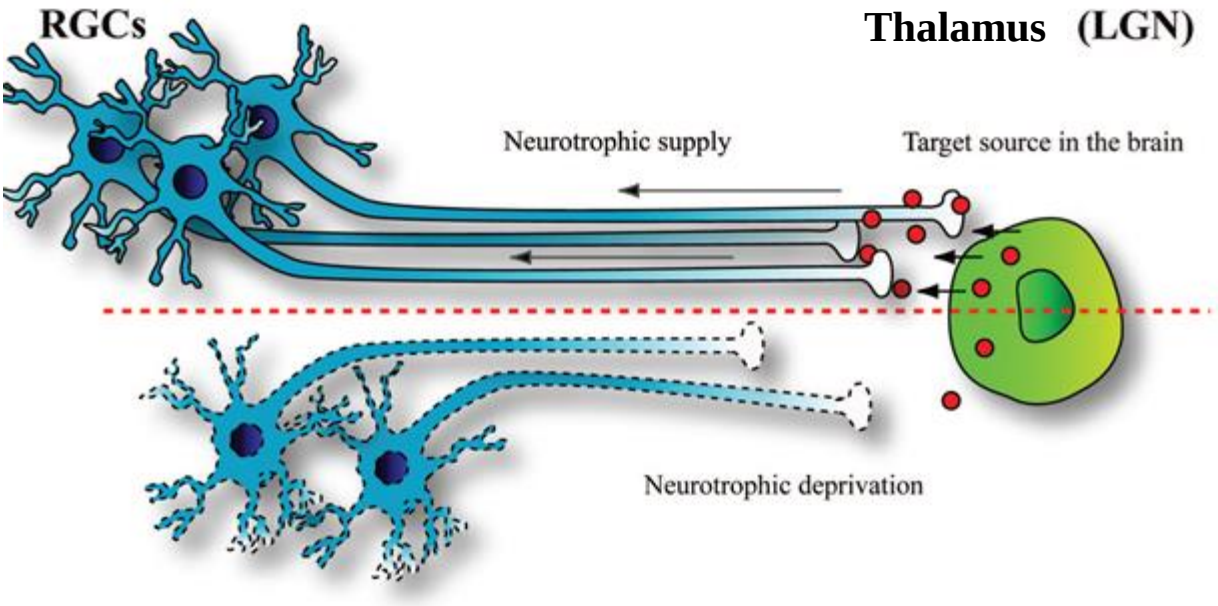

Figure 5: Neurotrophic supply from the target neurons in the brain sustain retinal ganglion cell survival: In glaucoma, both retro- and anterograde axonal transport of neurotrophic factors leads to progressive RGCs degeneration. Di Polo. (2008) [19]

Ischemia can lead to mitochondrial dysfunction by hypoxia, which increases the production of reactive oxygen species (ROS). The imbalance between the endogenous cellular antioxidant enzymes and the reactive oxygen species produced by the mitochondria cause ganglion cells to undergo apoptotic death. [21, 25] Moreover, mitochondrial dysfunction also causes depletion of the energy resources for axonal transport, also leading to ganglion cell degeneration. [5, 9, 19, 21]

Glutamate Excitotoxicity

Since, retinal ganglion cells, bipolar cells, and photoreceptors all use glutamate as their neurotransmitter, excitotoxicity due to the release of glutamate stores from dying neurons also has been proposed as a mechanism underlying progressive retinal ganglion cell degeneration in glaucoma. [5, 10, 25] The increased stimulation of ganglion cells by glutamate leads to excess calcium influx, activation of intracellular endonucleases and proteases, mitochondrial dysfunction, increased ROS production, and eventually cell death. [10]

Reactive Gliosis

Astrocytes, microglia, and Müller glia maintain homeostasis in the retina via the regulation of ion exchange, glucose levels, and transport of neurotransmitters. [9] In glaucoma models, these cells become activated by the injury, which leads to morphological changes (e.g. hypertrophy of glial soma and thickening of their processes, and transport dysfunction). In addition, they also may release the pro-inflammatory cytokine, tumor necrosis factor alpha (TNF-α). The excessive production of TNF-α induces cell death by interaction with TNF-R1 receptor causing induction of caspases 8 and 3. [4, 9, 21] Dysfunction of Müller cells decreases their ability to clear the excess glutamate released from degenerating neurons, leading to overstimulation of neighboring ganglion cells and activating Müller cells to enhance their production and release of TNF-α. [10] Disruption of mitochondrial respiration results in the production of increased levels of nitric oxide (NO) by astrocytes and microglia. [4, 10] Astrocyte dysfunction also leads to remodeling of the extracellular matrix of the optic nerve head due to an increased production of metalloproteinases (MMPs), matrix degrading enzymes.[9, 10] Therefore, the excessive production of MMPs leads to a

diminished ability of the LC tissues to resist the mechanical strain imposed against it by elevation of IOP. [4]

MECHANISMS OF RGC DEATH

Whatever the initial mechanism of the injury in glaucoma, the cellular process of retinal ganglion cell death is considered to be primarily by apoptosis. [4, 5, 9] Apoptosis (programmed cell death) is a highly regulated process of cell death characterized by shrinkage of the cell body, condensation of the chromatin, 'ladder-like' DNA fragmentation, and fragmentation of the cytoplasm and nucleus into membrane bound bodies that are removed by phagocytosis without having a negative effect on adjacent neurons (Fig. 6-B). By contrast, necrosis is characterized by cell body swelling, a vacuolated cytoplasm, breakdown of cellular organelles, and eventual rupture of the cell membrane, resulting in the release of the cellular contents, inflammation, and secondary degeneration of neighboring cells (Fig. 6-A). [5, 26, 27]

Programmed cell death of the retinal ganglion cells in glaucoma can be initiated by either the extrinsic (i.e. FAS ligand, TNF-α) or intrinsic (deprivation of neurotrophic factors) apoptotic pathway. Both result in activation of pro-apoptotic signaling pathways (e.g. BAD, BAX) and suppression of pro-survival signals (e.g. Bcl-2, Bcl-xl), leading to mitochondrial membrane permeabilization. This results in increased levels of ROS, decreased ATP, increased release of cytochrome C, and activation of the caspase cascade. [9, 26]

Autophagy is another cell death mechanism that has been suggested as being involved in glaucomatous RGC death. It is described as the natural self-degradation of unwanted or dysfunctional cell proteins and organelles by enclosing them in a double membrane vesicle (autophagosome) that fuses with lysosome, and results in the contents being degraded and recycled (Fig. 6-C). [5, 9, 26, 27]

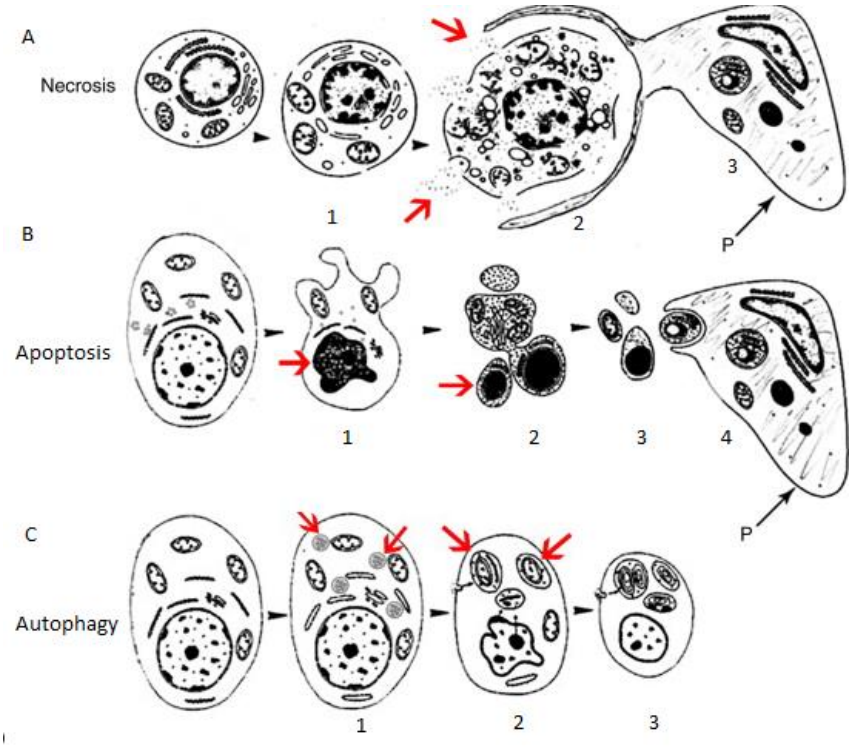

Figure 6: Cell death mechanisms: A) Cell necrosis is characterized by cell body swelling (1), vacuolated cytoplasm and cell membrane rupture (2), and eventually the cell is removed by Phagocytes (3) (P). B) The process of apoptosis begins with shrinkage of the cytoplasm and nucleus (1), fragmentation of the cellular contents into membrane bound bodies (2 and 3), and engulfment by phagocytes (4). C) Autophagy is characterized by formation of isolation membranes (1), enclosing the organelles in autophagosomes (2), and fusion of the autophagosome with a lysosome to be degraded. Modified from Chang et al. (2012) [26]

TREATMENT STRATEGIES

Whether by using topical medication or laser/surgical procedures, all current therapeutic strategies for treating glaucoma are limited to lowering the IOP. Unfortunately, IOP reduction only results in slowing, but not halting, progression of the disease. [4, 5, 9]

Topical medications: there are several IOP control medications that can be applied topically to the eye. [7-9, 28] Based on their mechanism of action they can be subdivided into medications that lower IOP by enhancing the outflow of aqueous humor through the trabecular meshwork, such as prostaglandins and cholinergic agonists, and those that reduce pressure by decreasing the production of aqueous humor via the ciliary body, such as carbonic anhydrase inhibitors and beta-adrenergic blockers. [8, 9, 28]

Although prostaglandins have the unique side effects of darkening the periocular skin and iris and lengthening the eye lashes, they generally are the first line of glaucoma treatment. Their primary mode of action is enhancement of aqueous outflow via the uveoscleral vs trabecular meshwork route through regulation of matrix metalloproteinases and remodeling of the extracellular matrix of these drainage channels of the eye. [9, 28] Cholinergic agonists, which increase aqueous outflow by causing contraction of the ciliary muscles, also may result in ocular side effects. These include dimming of vision due to pupillary constriction, as well as artificially-induced myopia. [9]

Carbonic anhydrase inhibitors and beta-blocker drugs, which reduce aqueous production by direct antagonist activity on the ciliary epithelial carbonic anhydrase and synthesis of cyclic AMP, respectively, have higher incidences of systemic side effects. Carbonic anhydrase inhibitors can

result in allergic reactions, as well as paresthesia of the fingers and toes, depression, gastrointestinal symptoms, and much more. [8, 9, 28] β-adrenergic receptor blockers can cause bradycardia, arrhythmia, bronchospasms, and fatigue, to name a few.

Adrenergic agonists also are used to control IOP. These act through alpha 2 adrenergic receptors primarily to mediate aqueous suppression via vasoconstriction, with a secondary mechanism (via cAMP production) that increases aqueous outflow. Common side effects include mydriasis, fatigue, tachycardia, and arrhythmia. [8, 9, 28]

Laser trabeculoplasty also is used for reducing IOP in open angle glaucoma, especially, for those patients with poor compliance to the topical medications [8]. The procedure involves applying laser energy to the trabecular meshwork in order to increase the outflow of aqueous humor [7-9]. For angle closure glaucoma, laser peripheral iridotomy is used to relieve the obstruction by creating a drainage opening in the iris. [7, 9]

Surgical intervention also is an alternative, and most often is used for refractory cases. [9] The two most common surgeries are trabeculectomy (partial removal of the trabecular meshwork) and insertion of a tube shunt devices that drains the aqueous humor to the subconjunctival space. [8]

Unfortunately, reduction of IOP decreases the risk of further progression of vision loss in glaucoma by only 17%, and thus new treatment strategies are required [8]. Since studies have indicated that a deficiency of neurotrophic factors (NTFs) and their receptors from the retina results in RGC death, administration of neurotrophic factors as a potential neuroprotective strategy to prevent or delay the disease progression is a promising strategy of glaucoma treatment, especially when used in conjunction with IOP lowering techniques. [30-44]

Primary members of the neurotrophic family include nerve growth factor (NGF), brain derived neurotrophic factor (BDNF), neurotrophins 3, 4, & 5 (NT3, N4/5), and ciliary neurotrophic factor (CNTF). [19, 45-47] Each has been shown to play an important role in neural survival and development by promoting activation of intracellular survival pathways and suppressing apoptotic pathways. [5, 30-44] With respect to the neurotrophins, all bind to the p75NT receptor with low affinity, but interact selectively with their distinct tropomyosin-related kinase receptor (Trk A, B, or C) with high affinity – NGF: Trk A; NT3: Trk A, B, C; BDNF/NT4/5: TrkB. CNTF has its own receptor. [5, 45-49]

BDNF

Among the various neurotrophins, BDNF has been characterized best with respect to its neuroprotective effects. [30-44] BDNF and its receptor (TrkB) are expressed widely in the mammalian central nervous system. [36] In the developing brain, BDNF expression reaches its highest levels by 10-14 days postnatal and gradually declines with age. [48] It plays important roles in neuronal development, morphogenesis, and cell differentiation. Blockage of BDNF signaling during early development results in abnormal patterning within visual cortex. [45] In the adult brain, BDNF expression distributes mainly in the hippocampus, cerebral cortex, cerebellum, and amygdala, and it has a critical function in neuronal survival and axonal growth. [45] *In vivo* application of BDNF has been shown to exert its neuroprotective effects on a variety of neurons in both ischemic and traumatic injury models. [29, 30, 31, 36-44]

BDNF is translated as a precursor protein (preproBDNF) in the endothelial reticulum, where it undergoes post translational modification to yield a proBDNF protein (32-KDa). ProBDNF is stored in the Golgi apparatus, in which the proBDNF is converted to mature BDNF (14-KDa) via endoproteases. Conversion to the mature form also can occur extracellularly under the effects of tissue plasminogen activator. Subsequently, the cell releases the mature BDNF, either passively as small vesicles that bud off from the Golgi apparatus and fuse to the cell membrane, or by an active process where the vesicles release their content following depolarization of the cell (Fig. 7). Neurons also can release the proBDNF protein, which binds to the NTp75 receptor and promotes apoptosis. More commonly, however, the mode of activity is the mature BDNF binding to the TrkB receptor and the BDNF-Trk receptor complex then being internalized and

transported either anterogradely or retrogradely along the axon to the axon terminal or cell body, respectively, where it activates intracellular signaling pathways. [45, 47, 51]

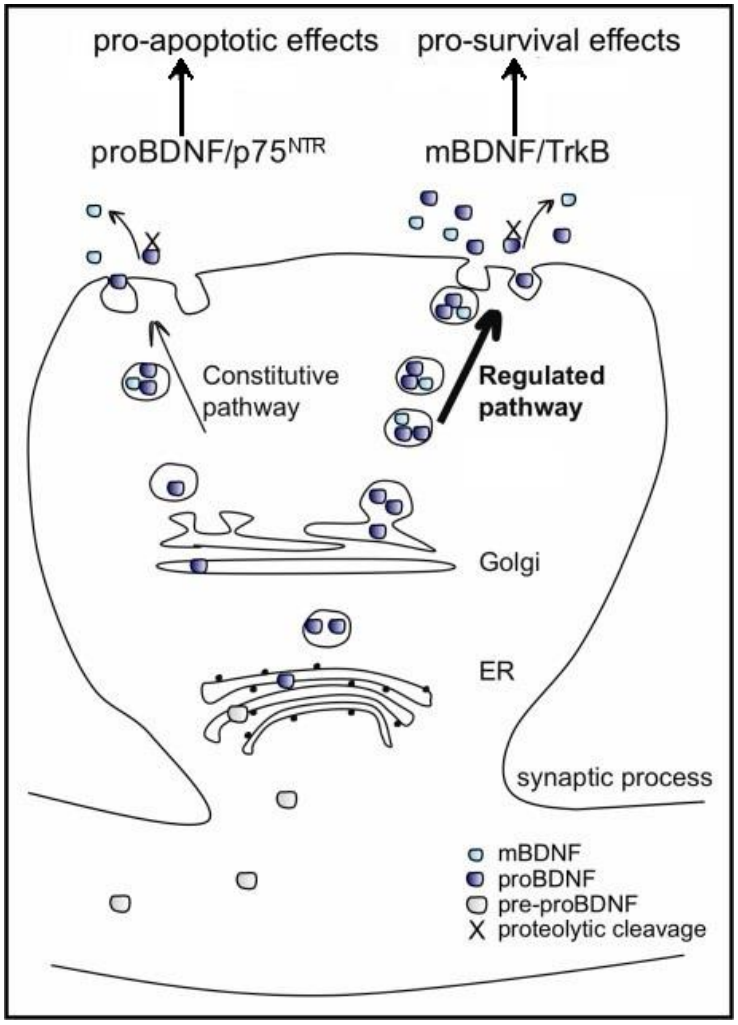

Figure 7: BDNF transport and trafficking: The precursor pre-proBDNF is modified in the reticulum endothelium ER to pro-BDNF. In the Golgi apparatus some of the pro-BDNF is converted into mature BDNF. Pro-BDNF and mature BDNF are released either by a constitutive pathway (passive), or by a regulated (active) pathway. Pro BDNF can be converted to mature BDNF extracellularly by proteolysis. The released Pro-BDNF can bind to the NTp75 receptor to promote apoptosis while mature BDNF binds to the TrkB receptor and promotes activation of anti-apoptotic pathways. Modified from Cunha et al. (2010) [62]

BDNF Signal Transduction

Binding of BDNF to its receptor activates several small G- proteins including Ras, Raf and Rho family members that lead to stimulation of multiple pro-survival signaling pathways (Fig. 8). These include both the mitogen-activated protein kinase (MAPK/ERK) and phosphatidylinositol-3 kinase (PI3K/AKT) pathways. The MAPK/ERK pathways activate the cAMP response element binding protein (CREB), a nuclear factor that promotes transcription of several pro-survival genes, including *BCL2* and *BCL-XL*. The PI3K/AKT pathway also results in activation of CREB, but it also acts to preserve mitochondrial function via direct promotion of the anti-apoptotic protein BCL-2 and inactivation of the pro-apoptotic protein BCL-2 Associated Death promoter (BAD), thus preserving the mitochondrial membrane potential and preventing release of cytochrome c and activation of neurodestructive caspases. [19]

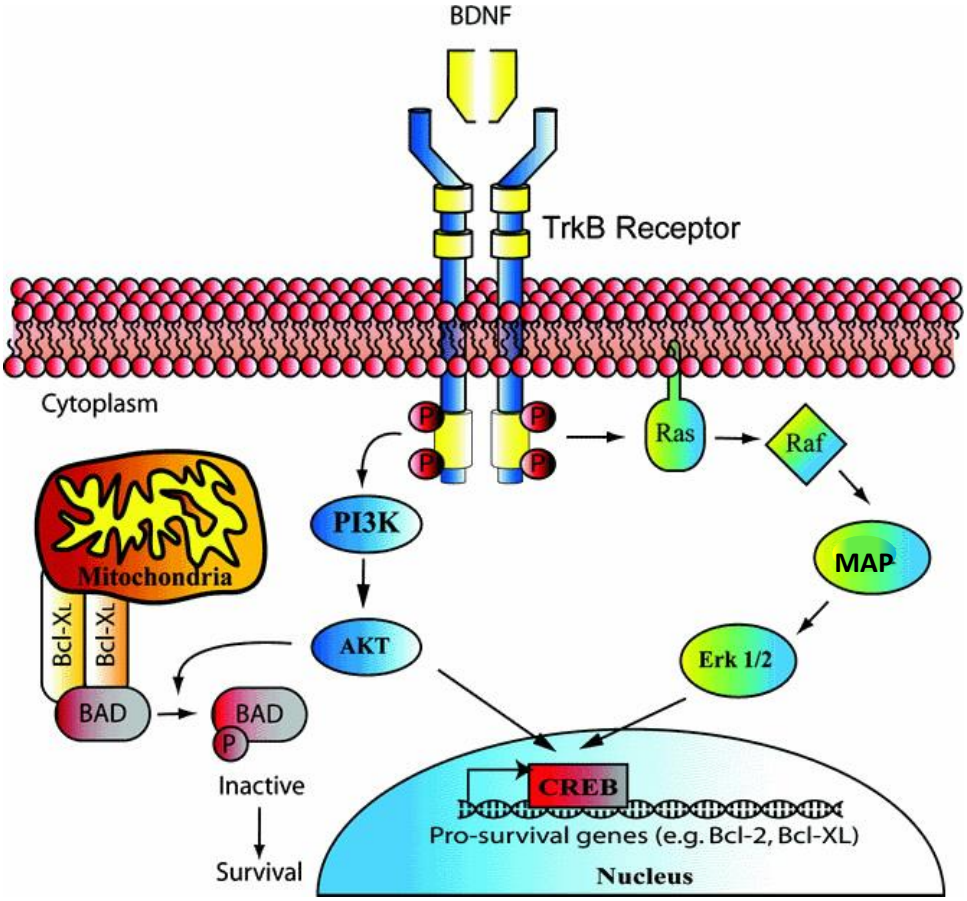

Figure 8: BDNF signal transduction: BDNF binding to the TrkB receptor promotes a series of pro-survival pathways. Receptor phosphorylation and activation of Ras results in activation of the mitogen-activated protein kinase (MAPK)-signaling cascade and phosphoinositol-3 kinase (PI3K)/protein kinase B (AKT) pathway. Activation of the MAPK/ERK pathway promotes the cAMP response element binding protein (CREB), which promotes transcription of pro-survival genes. Activation of phosphoinositol-3 kinase (PI3K)/protein kinase B (AKT) pathway promotes cell survival via activation of CREB along with in-activation of the pro-apoptotic protein Bcl-2 Associated Death promoter (BAD). Modified from Di Polo. (2008) [19]

BDNF AND RETINAL GANGLION CELLS

Over the past few years several experimental approaches involving BDNF treatment have been used to promote RGCs survival after optic nerve damage. Despite the potent neuroprotective effect of direct injection of BDNF into the injured eye, this approach to date has failed to sustain significant RGC survival for more than 7 days, even with multiple applications. The inability of BDNF to provide sustained levels of neuroprotection is thought to result from a down-regulation of TrkB receptors in the treated eye due to over exposure to the injected BDNF. [19, 30, 31] To overcome this problem of receptor down regulation, injection of BDNF into the eye has been combined with transfection of the TrkB receptor gene into retinal ganglion cells using recombinant viral vectors, as well as by transplantation of engineered mesenchymal stem cells into the eye to secrete BDNF in a slower and more sustained manner. [29, 48] While these approaches have resulted in modest increases in the number of surviving ganglion cells, their continued failure to show long term neuroprotection might also be attributed to the fact that in all cases the nerve injury model used resulted in a complete separation of the retinal ganglion cells from their target neurons in higher visual centers. [31] Thus, by limiting their treatment only to the eye, these studies disregarded the contribution that trophic materials derived from retinal target neurons in higher visual centers play in RGC health and survival. Evidence from experimental primate and human glaucoma suggests that neurodegenerative changes extend from the eye and optic nerve to visual centers in the brain. Thus, changes in the levels of trophic materials in these centers may contribute to the pathology of glaucoma, but also might serve as an avenue for therapy (Fig. 9). [12, 49, 50]

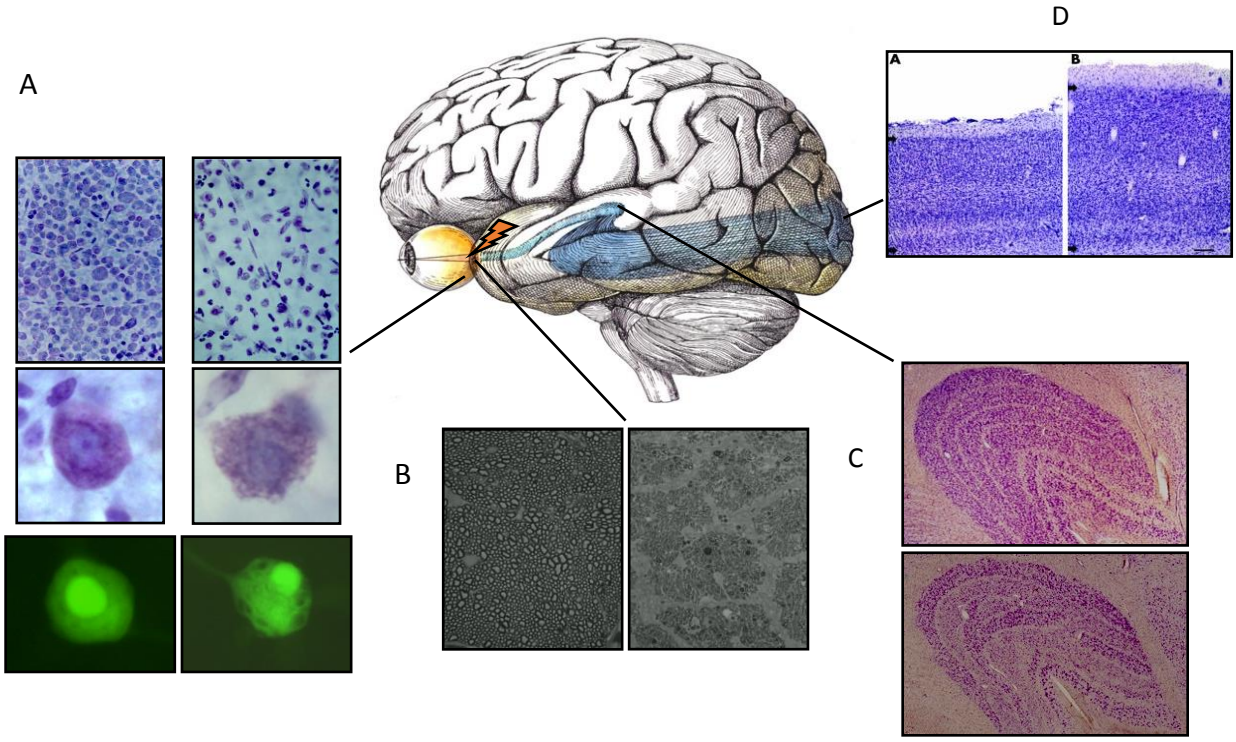

Figure 9: Histopathological changes in the glaucomatous eye: A) Upper: Photomicrographs of cresyl-violet stained monkey retinas showing decreased ganglion cell densities in the sample regions of the glaucoma model retina (right) in comparison with a normal retina (left). Middle and lower: high power view of the morphologies of retinal ganglion cells from the glaucoma eye (right) showing irregular surface contour of the cell body, eccentric placement of the nucleus, and vacuolated cytoplasm, indicating its degeneration. Weber et al. (1998-2000) [63, 64] B) Comparison of cross sections of a normal nerve (left) that shows uniform staining, clear myelinated axons, and thin septae separating the axon bundles and a glaucomatous nerve (right) showing uneven staining and dark degenerative axon profiles. Weber et al. (2001) [65] C) Photomicrographs of coronal sections from the left LGN of a normal monkey (upper) and an animal that had the pressure in one eye elevated (lower). In the glaucoma animal the layers innervated by the glaucomatous eye show a significant decrease in neuronal size and content of Nissl substance within their cytoplasm, resulting in their pale appearance. Weber et al. (2000) [64] D) The visual cortex (Nissl stained) from a human with glaucoma (left) shows marked thinning of the cortical layers compared to the normal cortex (right). Gupta et al. (2006)

In agreement with this hypothesis, recent work in our laboratory has demonstrated that a single application of BDNF to the eye combined with chronic infusion of BDNF to visual cortex, which has an extensive reciprocal relation with the visual thalamus, not only enhances retinal ganglion cell survival and function after a mild optic nerve injury in the cat, but that it also provides a neuroprotective effect that lasts at least 6 weeks (longest period studied), even when the cortical treatment is discontinued after 2 weeks post nerve injury (Fig. 10). [31, 32] Treatment of visual cortex alone was not found to be beneficial, most likely for two reasons: First, because of the delay in time for the BDNF to be transported, both anterogradely and retrogradely, to the visual thalamus, the primary target of retinal ganglion cells, and 2) because the injury occurs very close to the eye, it exerts its degenerative effects on the retina very rapidly. Therefore, direct application of BDNF to the eye is essential to sustain RGC survival during the period immediately post injury until the cortical applied of BDNF can exert its protective effects – the intraocular injection provides about a 1 week window of significant protection.

Further support that transport delay might underlie our failure to achieve retinal neuroprotection following application of BDNF to visual cortex alone is supported by the work of Frost et (1998).[30] They injected BDNF into the superior colliculi of newborn hamsters and compared the level of RGC loss that occurs naturally at different time periods post-injection. At 8 hrs. post-injection there was no difference in ganglion cell loss between the normal and injected animals, whereas at 20 hrs. post-injection there was a significantly greater number of surviving neurons in the BDNF injected animals. In the previous studies, a brain infusion cannula connected to an osmotic mini-pump was used to deliver the recombinant BDNF into visual cortex.

As noted, such exogenous application of drug has the potential of overwhelming the local

TrkB receptors, leading to their down-regulation, and a decrease in the level of neuroprotection. [31, 32] In the present study, we sought to overcome this potential by using an optogenetic approach to induce the cells in visual cortex to produce endogenous levels of BDNF sufficient to yield long-term preservation of retinal ganglion cells and function after a mild optic nerve injury in rats.

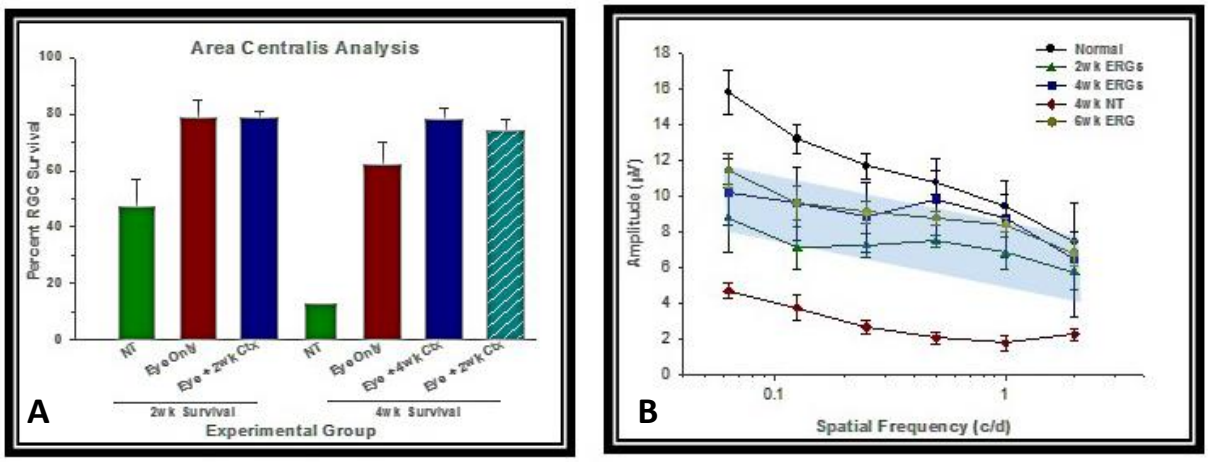

Figure 10: Brain infusion to deliver recombinant BDNF into visual cortex combined with BDNF eye application enhances retinal ganglion cell survival and function in cats with optic nerve damage: A) Comparison of the percent ganglion cell survival in the area centralis (AC) for cats receiving different treatment strategies, and either 2- or 4- week survival periods. At 2 weeks after injury/treatment, there was a significant increase in ganglion cell survival following treatment of the eye alone and the combined eye and visual cortex ($P < 0.05$) compared to no treatment (NT). Following a 4-week survival period, all treatment conditions enhanced ganglion cell survival significantly relative to NT ($P < 0.05$), with the dual treated animals (DT) showing a significant increase over those receiving treatment of the eye alone ($P < 0.05$). Although those receiving only 2 weeks of treatment, followed by an additional 2-weeks without treatment, showed a slight reduction in ganglion cell survival in the AC, they were not different from those animals receiving 4 weeks of treatment ($P > 0.05$), suggesting that 2 weeks of cortical treatment might be sufficient to preserve a significant number of retinal ganglion cells. B) Pattern ERG responses to gratings of different spatial frequency for normal animals, animals that received no treatment, or those that received 2 weeks of dual treatment to the eye and cortex followed by either 2, 4, or 6 week survival period. Although not normal, the responses measured in the treated animals are significantly better than those measured in animals not receiving treatment. Note also that the 4, 6-week DT responses are consistently stronger than the 2-week DT responses. Weber et al. (2010-2013) [31, 32]

OPTOGENETIC APPROACH TO ENDOGENOUS NTF PRODUCTION

Artificial neuronal stimulation can be achieved by several different techniques. Electrical stimulation using extracellular electrodes has limitations because of its low spatial resolution and electrical interference between the electrode and neuronal tissues. Pharmacological stimulation of neurons, with or without genetic manipulation, is limited by their slow kinetics and poor reversibility. The optogenetic approach provides high spatial and temporal resolution, and ease of reversibly stimulating neurons with millisecond resolution. [51-54]

As the name implies, optogenetics is based on the use of genetic methods to induce neurons to express photosensitive proteins, which then allows one to control their neuronal activity using different wavelengths of light. For the most part, these light sensitive proteins have been isolated from various algae and bacteria. [52-54] The one we selected to employ for these studies is Channelehodopsin-2 (ChR2), which provides the green algae Chlamydomonas reinhardtii with its phototaxic ability. The construct contains the human synapsin 1 gene promoter and m-cherry fluorescent tag for the identification of transfected cells. It is delivered via a recombinant human adeno-associated viral vector (Fig. 11). The total construct is: (rAAV2/hSyn-hChR2(H134R)-mcherry). Stimulation of the transfected cortical cells with blue light (~470 nm) results in the opening of non-specific, ionotropic, cation channels and excitation of the neurons. Deactivation time is about 12-18 ms. [52, 54]

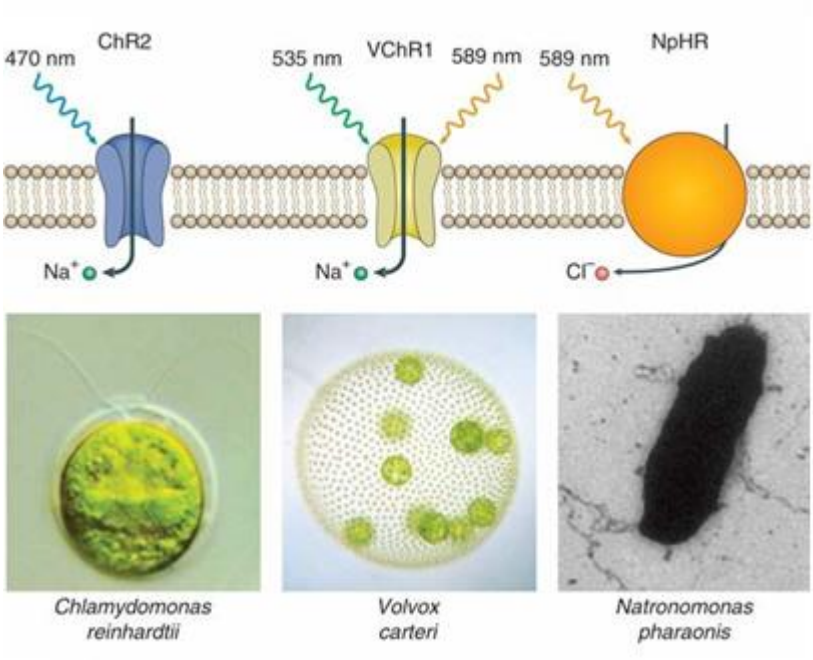

Figure 11: Three examples of light sensitive proteins widely used in optogenetics: Channelrhodopsin (ChR2) from Chlamydomonas reinhardtii and Channelrhodopsin ChR1 from Volvox carteri are light-sensitive, membrane-bound cation channels that open with stimulation via a specific wave length of light, to produce depolarization of the expressing neuron. Halorhodopsin (NpHR) from Natronomonas pharaonis is a light sensitive chloride pump that is activated by yellow light to hyperpolarize the expressing neuron. Deisseroth, (2011). [53]

METHODS

SUBJECTS AND GROUPS

All surgical procedures and experimental protocols were reviewed and approved by the Institutional Animal Care and Used Committee at Michigan State University and all adhered to the Association for Research in Vision and Ophthalmology (ARVO) Statement for the Use of Animals in Ophthalmic and Vision Research. Twenty Sprague Dawley rats (300-650g) of both sexes were randomly separated into four groups. Animals in the Control Group were handled similar to those in the experimental groups, but did not undergo any procedures. These animals provided the baseline values for normal RGC number and density. A second group of animals underwent a controlled optic nerve crush procedure, and served as the baseline for RGC loss following optic nerve injury without treatment. The third group of animals underwent optic nerve crush and received a single, intravitreal, injection of BDNF to the affected eye at the time of the nerve crush, and thus served as the baseline for the neuroprotective effect of treatment of the eye alone. The fourth group of animals underwent the optic nerve crush procedure and intraocular BDNF injection, combined with optogenetic stimulation of the contralateral visual cortex daily for 9 days. All experimental animals received a 9-day post-nerve injury survival period, as previous nerve crush studies in the rat have shown this to be a period at which there is a moderate, but not severe loss of retinal ganglion cells. [9, 37, 55, 56]

SURGICAL PROCEDURES

Optic Nerve Crush and Intravitreal BDNF Injection

Anesthesia for both procedures was induced with an intramuscular injection of ketamine (8 mg/kg) and xylazine (7.5 mg/kg). Analgesia consisted of a subcutaneous injection of meloxicam (2.5 mg/kg), and hydration was maintained with a subcutaneous injection of sterile saline. Body temperature was maintained at 37^0 C with a water-based heating pad. The region along the lateral canthus of the left eye was shaved and the area scrubbed with non-detergent betadine solution. The eyes then were treated with 0.5% proparacaine HCl (Henry Schein Animal Health, Inc.) and 2.5% hypromellose (Goniovisc™, HUB Pharmaceuticals Rancho Cucamonga, California, USA), to prevent corneal drying. To minimize exposure of the retina to the microscope light, the eye undergoing surgery was covered with a small section of a powder free purple nitrile examination glove. Using sterile procedures, the tissue of the lateral canthus was clamped with a straight hemostat for 5-10 sec. to minimize bleeding, and an incision was made that extended caudally for approximately 1 cm. Following blunt dissection of the lateral rectus muscle and removal of the orbital fat, the optic nerve was exposed. A vascular clamp then was placed on the optic nerve approximately 0.5-1 mm behind the posterior pole of the eye for 15 sec. Following the nerve crush a small piece of sterile saline soaked Gelfoam was placed behind the eye, the lateral canthus was closed with sterile suture, and the external area treated with betadine. Post-surgery, the animals were placed on a heating pad to recover before being returned to the animal care unit.

For BDNF injections, recombinant human BDNF (5µl @ 1µg/µl; PeproTech) was injected into the vitreal chamber. All injections were made using a Hamilton syringe with a 34-gauge needle. All injections were made approximately 2.0 mm posterior to the limbus, over a one-minute period, with the needle left in place for an additional 30 sec. to allow time for diffusion of the drug away from the injection site. No significant backflow was observed on retraction of the needle. A glass coverslip was applied to the cornea during the procedure for better clarity of insertion of the needle, so as to avoid injury to other structures within the eye, such as the iris, lens, or retina, which have been shown to promote RGC survival.[39, 57] The eye then was treated with a sterile ophthalmic ointment containing neomycin, polymyxin B sulfate, and dexamethasone, and the rat was placed on a heating pad until it recovered from the anesthesia. Postoperative pain medication was provided as described above, and the rat was monitored every hour for the first 6 hrs., and then daily for the remainder of the survival period. All procedures were performed on the left eye with the right eye serving as an internal control.

Optogenetic Procedures

For the AAV injections, anesthesia was induced with 4 % isoflurane (IsoFlo; Abbott Laboratories, Abbott, IL) delivered in pure O_2 at 2L/min. and maintained using 1.5-2.0 % isoflurane delivered at 0.8L/min. Using a stereotaxis and sterile surgical procedures, a 2.0 cm midline incision was made in the skin overlying the skull. The center of the right visual cortex was determined relative to Bregma at AP -6.3 mm; ML 3.4 mm. Using a micro drill (Ideal), a small opening was made at the center point, and another pair of openings made approximately 1.0 mm anterior and posterior to the first. Using a Hamilton syringe with a 34-gauge needle, 1.0 µl

of an adeno-associated viral vector containing channelrhodopsin-2 (ChR2) and mCherry genes (AAV-hSyn-hChR2(H134R) mCherry; UNC Vector Core) was injected at each cortical site at a depth of 0.7 mm from the surface of the brain. The injections were made in 0.5 µl increments over a 30 sec. period each, and the needle was left in place for 10 min. before injecting the second 0.5 µl with a similar post-injection waiting period to allow for the virus to diffuse away from the injection site. Following the last injection, the holes were sealed with bone wax and the skin overlying the skull was sutured and treated with betadine and 2.0% lidocaine gel. The animals then received subcutaneous fluids and analgesia, as noted above, and were placed on a heating pad to recover.

The animals scheduled for optogenetic stimulation received their optic nerve injury and intravitreal BDNF injection the same day they were prepared for cortical stimulation. For optogenetic cortical stimulation, at least 3 wks. post-injection of the virus to allow for optimal cortical transfection, the animals were re-anesthetized and placed back into the stereotaxis. After removing the bone wax used to seal the injection sites, a 1.5 mm wide groove connecting the three original openings was made to provide a larger area for cortical stimulation. This injection/stimulation process was used because making a larger opening as part of the initial surgery resulted in tissue and blood vessel growth over the opening at 3 weeks, which then made it difficult to obtain a clear exposure of the cortex for stimulation. A chamber, fashioned from a 1.0 ml tuberculin syringe, was attached to the skull with two stainless steel screws and the chamber-skull seam sealed with light-sensitive super glue. The chamber served as a port for insertion of the light emitting diode (460 nm; Cree TR2227; Cree, Inc.) used to activate the transfected neurons in the visual cortex *in vivo*. The incision around the chamber was sutured

and treated with betadine and 2.0 % lidocaine gel. Animals were given pain medication (meloxicam 2.5 mg/ kg) and fluids subcutaneously, and placed in a cage on a heating pad to recover. Animals were stimulated for 45 min. daily over their 9 day survival period.

ERG RECORDINGS

The flash ERG records global retinal activity after presentation of a light stimulus. Major components of the ERG are used to assess the function of specific neuronal populations within the retina (Fig. 12). In the photopic (bright light) ERG the a-wave is generated by photoreceptors and the b-wave is generated primarily by ON-bipolar cells, with lesser contributions by amacrine and Müller glial cells. In the rodent scoptopic (dim light) ERG, the pSTR reflects primarily the responses of ganglion cells while the nSTR is due primarily to the responses of amacrine and ON-bipolar cells. [82,83, 89]

For examination of visual function, an additional 11 animals (4 each: crush; crush+eye treatment; and 3 animals with crush+eye treatment+optogenetic stimulation) were prepared and their scotopic threshold responses (STR) measured prior to and following the prescribed survival period. The rats were dark adapted overnight and all preparations for recording were performed under dim red light illumination. Animals were initially anesthetized with 4.0% isoflurane delivered in pure O_2 at 2.0 L/min and were maintained using 1.5-2.0% isoflurane and oxygen delivered at 0.8 L/min. Their pupils were dilated using 2.5% phenylephrine (Paragon Pharmaceuticals, LLC) and 1.0% tropicamide (Akorn, Inc.) The animals were placed on a heating pad to maintain body temperature. A reference electrode was placed on the animal's tongue, and a ground electrode (Grass Technologies, Warwick RI) was placed subcutaneously over the dorsum. A contact lens corneal recording electrode (Mayo, Japan) was placed on each eye using a thin layer of hypromellose ophthalmic demulcent solution to maintain contact between the cornea and the electrode and to decrease recording noise. ERGs were recorded with an Espion

E2 electrophysiology system with ColorDome Ganzfeld (Diagnosys LLC, Lowell, MA, USA) using a dark-adapted luminance-response series of -4.0 to -2.4 log cd.s/m^2.

The pSTR, representative of ganglion cell function, was analyzed for each stimulus and was measured from baseline to the peak of the positive deflection, at approximately 110 ms from the flash onset. The pre-and post-treatment responses were compared for each eye, as well as the responses of the treated eye with its fellow non-treated eye. ERG wave amplitudes were measured for each animal group and the mean ratio difference between the experimental and control eyes pre- and post-treatment were obtained for each stimulus intensity (mean ± SD). Descriptive statistics were calculated, t-test was used for the comparisons between the response of both eyes prior and post-crush in each experimental group. ANOVA tests were used to compare the percent response between different animal groups followed by the Bonferroni test for multiple comparisons. The statistical significance was placed at $p < 0.05$ for all tests.

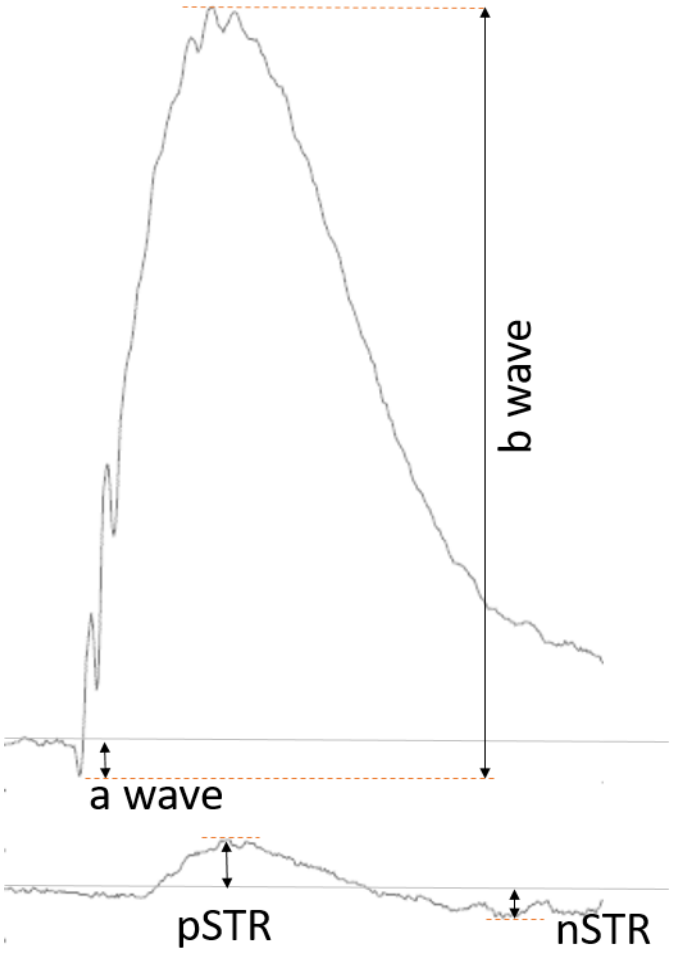

Figure 12: Major components of the electroretinographic traces in a normal rat in response to flash stimuli: In the photopic (bright light) ERG, the initial negative wave is the a-wave, which is generated by the photoreceptors. The second, positive-going wave is the b-wave, measured from the bottom of a-wave to its peak. It is generated primarily by ON-bipolar cells. In the rodent scotopic (low light) ERG, the pSTR reflects predominantly the responses of the ganglion cells while the later occurring nSTR reflects primarily amacrine and ON-bipolar responses. [89]

HISTOLOGY

All animals were euthanized with an i. p. injection of heparin followed by an overdose of pentobarbital sodium. Animals receiving optogenetic stimulation of visual cortex received a post-stimulation survival period of either 90 min. or 4 hrs., depending on whether they would be used for immunohistochemical demonstration of c-Fos, an indicator of neuronal activity, or BDNF expression, respectively. All were perfused transcardially with 4% paraformaldehyde in 0.1 M phosphate buffer (pH 7.4). Following perfusion, the brain was exposed and the head immersed in the same fixative at 4^{o}C for at least 24 hr. The stimulated region of each brain was cut into serial 50 µm coronal sections using a Vibratome (Lancer) and processed for immunohistochemical analyses.

For demonstration of c-Fos expression, the brain sections first were soaked for 2 hrs. at room temperature in 1.0% normal goat serum in phosphate-buffered saline (PBS) in order to block non-specific binding. Next they were incubated over night with primary antibody (rabbit anti-c-Fos 1:500; Cell Signaling Technology mAb 2250s in 0.3% Triton X-100/ PBS at 4 °C). The sections then were washed with PBS containing 0.1% Tween-20 three times, and incubated with the secondary antibody, AlexaFluor 488 goat anti-rabbit IgG (Life Technology) diluted 1:1000 in PBS + 0.1% Tween-20 for 2 hrs. at room temperature. Finally, the sections were washed with 0.1M sodium phosphate buffer, mounted onto glass slides using anti-fade mounting media (Vector Labs), and cover slipped. The sections were viewed with a fluorescent microscope to compare labeling between the stimulated and non-stimulated visual cortices.

For demonstration of BDNF expression, the endogenous peroxidase was blocked with 1.2% hydrogen peroxide in distilled water for 5-10 minutes. After washing in PBS, the sections were pre-incubated for 1 hr. at room temperature in the blocking serum (1.5% normal goat serum in PBS) to eliminate non-specific staining. Next they were incubated with primary antibody (rabbit anti-BDNF 1:100; Santa Cruz sc546 in the blocking serum for 48 hrs.). After rinsing in PBS, the sections were incubated for 30 minutes at room temperature with biotinylated goat anti-rabbit IgG (SantaCruz rabbit ABC staining system: sc-2018) at a dilution of 1:200 in the blocking serum. Following rinsing with PBS, the ABC complex (1:1 Avidin: biotinylated horseradish peroxidase) at a dilution of 1:50 in PBS was applied for 30 min. Following washing with PBS, sections were incubated in peroxidase substrate and DAB chromogen for 1–5 min until the color was developed. Finally, the sections were dehydrated in graded alcohol, mounted onto glass slides, cover slipped, and viewed with light microscope for BDNF staining comparison.

The retinae were prepared for retinal ganglion cell counting by immunofluorescent staining for RBPMS, a selective marker of RGCs.[58] After dissection from the eye cup, the isolated retinae were washed with PBS for 30 min., followed by soaking in 0.3% Triton X-100/PBS for 2 hrs. They then were soaked in 10% normal goat serum/0.3% Triton X-100/PBS for 2 hrs. at room temperature in order to block nonspecific binding. Next they were incubated with the primary antibody (rabbit anti-RBPMS; GeneTex; 1:200) in 10% goat serum/0.3% Triton X-100/PBS at 4^{o} C for 5 days. The retinae then were washed with PBS every 20 min. for four hrs. and incubated with AlexaFluor 555 goat anti-rabbit IgG secondary antibody diluted 1:1000 in PBS + 0.1% Triton X-100 for 48 hrs. at 4^{o} C. Finally, they were washed in PBS for 2 hrs. The retinae then were whole-mounted, ganglion cell layer up, onto gelatin-coated glass slides, and coverslipped with anti-fade

mounting medium containing DAPI (Vector Labs). The retinae were viewed with a fluorescent microscope for the capture and counting of retinal ganglion cells.

Optic nerve segments from each eye were obtained 2-3 mm posterior to the globe. Optic nerves were post-fixed with 2.5% paraformaldehyde and 2% glutaraldehyde for at least 24 hrs., then for 6 hrs. in 1% osmium tetroxide in dH_2O. Following post-fixation, the nerves were dehydrated in graded alcohols and embedded in epoxy resin (LX-112; Ladd). Cross-sections (1 μm) were cut with an ultra-microtome, mounted on glass slides, and stained with toluidine blue.

Ganglion Cell Measurements

Topographical analysis of RBPMS immunolabeled cells was performed using a Nikon FX-A fluorescent microscope and 20 x objective. Each retina was divided into four quadrants. Three, non-overlapping, regions of approximately $1.7x10^5$ μm^2 were imaged with a computer-based imaging system at each of 3 distances (1, 2, and 3 mm) from the optic disk for each retinal quadrant – 36 total sample regions, total sample area of approximately 6.12×10^6 μm^2, or 15% of the total area of the average rat retina (Fig. 13). In each region, the number of RBPMS-positive cells was counted directly from the digital images with image analysis software (iVanya; Antonov, Ivan. "Visual Counter on the App Store." App Store). Because of inter-animal variability, the percent survival was defined by the number of ganglion cells in the experimental eye versus those in the contralateral control eye of the same animal for each condition.

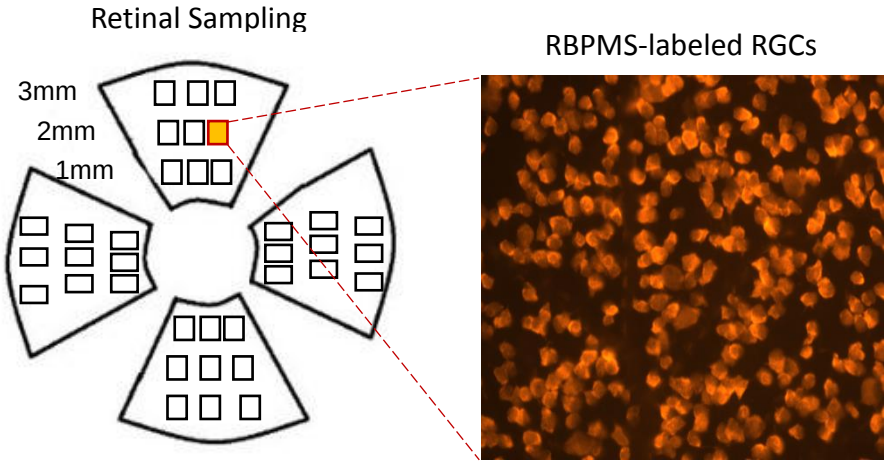

Figure 13: RGC sampling areas and RBPMS labeling: A) each retina was divided into four quadrants and each quadrant divided into three zones – central, middle, peripheral. Three sample regions were measured within each zone.

Optic Nerve Measurements

The degree of optic nerve damage was evaluated using a semi-quantitative grading scheme similar to that used by other investigators [59]. Optic nerves were assigned scores of 1 to 5 based on qualitative assessment of the level of nerve damage, with 1 representing a totally healthy optic nerve and 5 representing a severely damaged optic nerve. The nerve analyses were performed in a masked manner.

STATISTICAL ANALYSIS

All data are presented as mean ± SD. The retinal cell ganglion counts were normalized by dividing each measurement in each zone by the mean of the normal cell count in that zone and multiply it by 100. The percentage of the retinal ganglion cell count in the experimental eye to the normal fellow eye of the same animal, was determined and compared for all of the animals across the different experimental conditions using a one way ANOVA followed by the Bonferroni test for multiple comparisons. In all cases, $p=0.05$ was used as the level of significance.

RESULTS

VIRAL TRANSDUCTION OF ChR2 AND THE OPTOGENETIC ACTIVATION OF THE ADULT RAT VISUAL CORTEX

As a visible indicator of the level of neuronal transfection, and thus potential expression, of the ChR2 protein in visual cortex, we employed an AAV2 vector that combined the ChR2 gene with that for m-cherry, thus resulting in fluorescent labeling of the virally transfected neurons. Following a 3 week post-injection period, coronal sections of visual cortex showed expression of ChR2 across all layers within the injection site, as demonstrated by the distribution of m-cherry labeling. On average, the approximate range of transfected cortex extended about 1-1.5 mm from the center of each injection (Fig. 14).

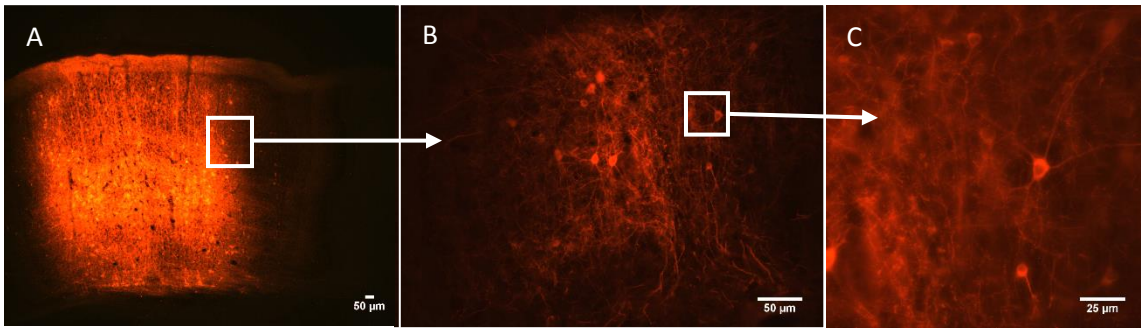

Figure 14: Virus transfection of ChR2: Coronal sections of visual cortex showing the spatial distribution of fluorescent m-cherry labeled neurons. Note that the label extends dorsal-ventrally across all of the cortical layers within the injection site. Higher magnification image shows staining of a few cell bodies with extensive labelling of the dendrites

As noted previously, in order to demonstrate that optical stimulation of the ChR2-transfected cortical neurons enhanced their electrical activity, immunohistochemistry for c-fos expression was used. To assess any potential direct effect of the virus alone, rats received bilateral virus injections but only unilateral light stimulation. A comparison of cortical c-fos labeling in the injected, but non-stimulated visual cortex versus the injected and stimulated cortex, is shown in (Fig. 15-A). While the virus did result in an increase in c-fos expression, this expression was highly restricted to the injection site. By contrast, c-fos expression in the stimulated cortex extended across all layers and was extensive in both the rostral-caudal and medial-lateral directions.

To confirm that optical stimulation selectively activates only the transfected neurons, we stimulated a wild type rat unilaterally using the same LED. The neurons of the stimulated side exhibited no enhancement of c-fos immunostaining compared with the non-stimulated side (Fig. 15-B).

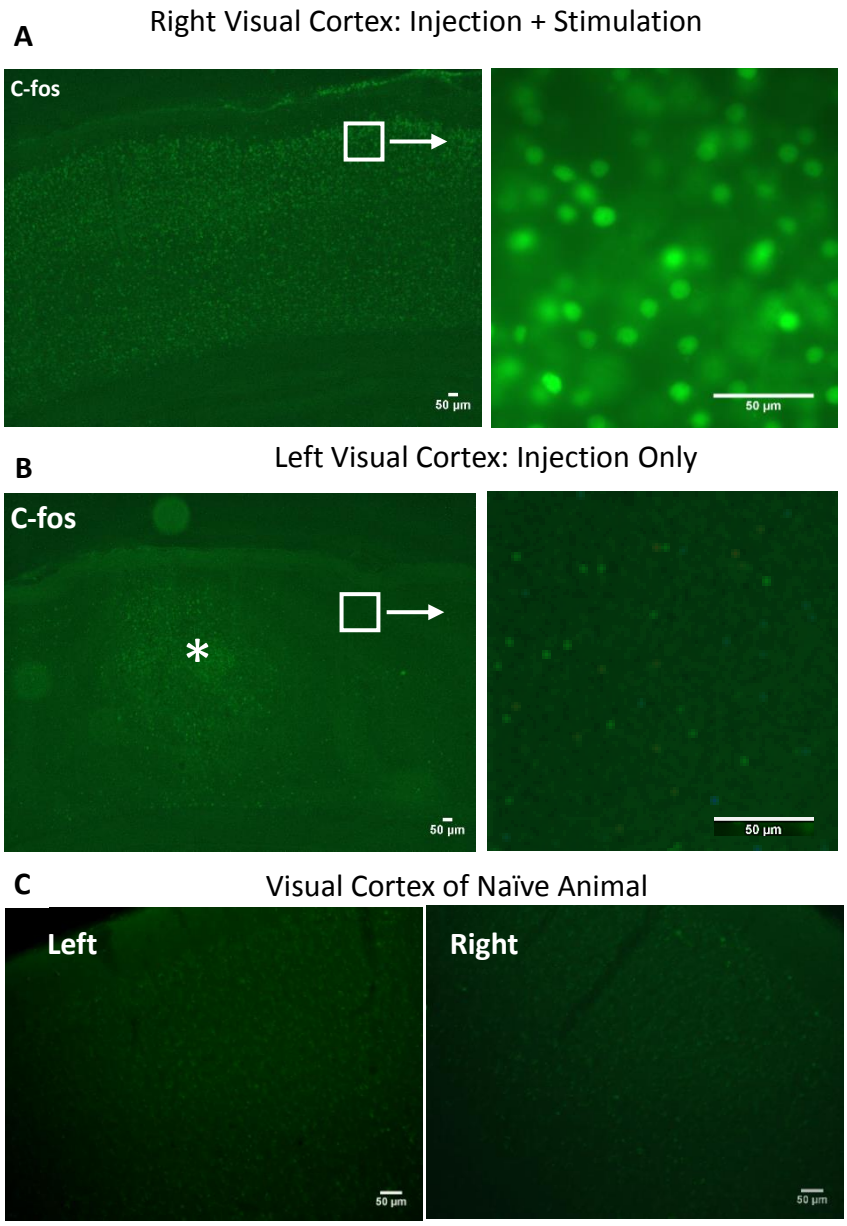

Figure 15: Neuronal activation by optogenetic stimulation: A) In vivo optogenetic stimulation of the visual cortex results in an overall increase in c-fos activity on the stimulated side in comparison with the non-stimulated side of bilaterally viral transfected rat. B) The spatial range of c-fos expression is restricted to the virus injection site (*) in the non- stimulated side. In contrast, on the stimulated side A, c-fos expression extends across all cortical layers and the mediolateral axis as well. C) Optical stimulation in a wild type, non-transfected animal, resulted in no differential neuronal excitation when comparing c-fos expression on the stimulated (right) vs non-stimulated (left) sides of visual cortex

ENHANCEMENT OF BDNF EXPRESSION VIA OPTOGENETIC ACTIVATION IN THE ADULT RAT VISUAL CORTEX

Previous studies from our lab have indicated that, following optic nerve injury, application of BDNF to both the eye and visual cortex is more beneficial than treatment of the eye alone. One goal of this study was to determine whether optogenetics could be used to induce endogenous expression of BDNF in visual cortex. Using a rat that received bilateral injections of the AAV2 virus and unilateral light stimulation, we processed the cortical tissue for BDNF immunohistochemistry. The tissue revealed increased BDNF expression in the stimulated cortex compared with the non-stimulated side. On the stimulated side, the BDNF expressing cells were more widespread than the non-stimulated side, where the few BDNF expressing cells were confined to the injection site. Interestingly, the enhanced BDNF expression appeared to be associated primarily with astrocyte-like cells (Fig. 16).

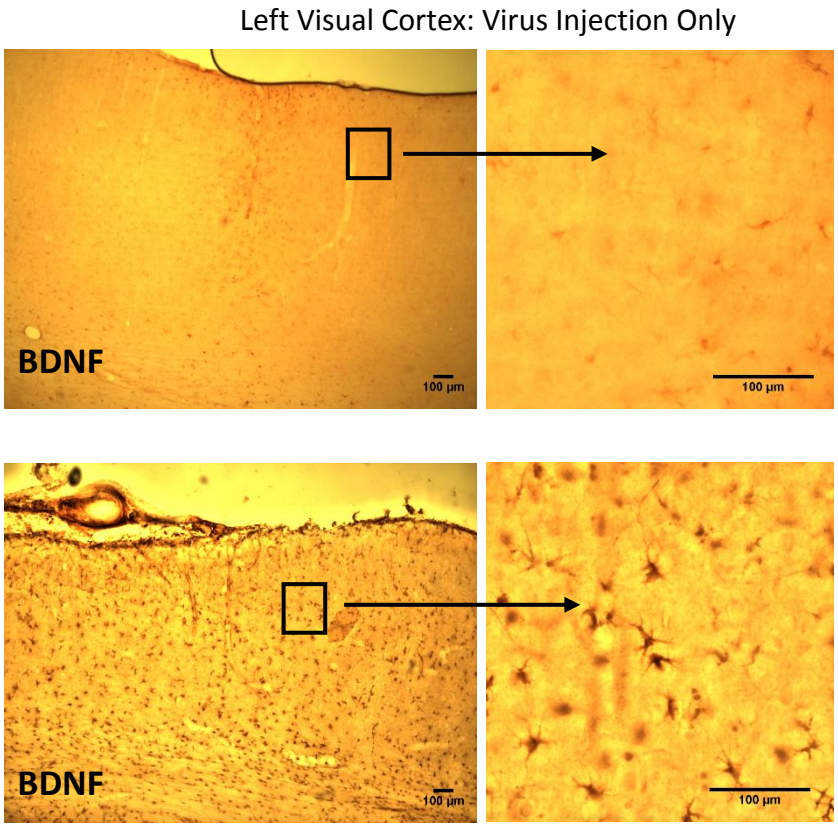

Figure 16: Enhancement of BDNF expression via optogenetic stimulation: Coronal sections of visual cortex showing increased BDNF expression in astrocyte-like cells across the cortical layers of the stimulated versus non-stimulated side of a bilaterally transfected rat.

GANGLION CELL SURVIVAL MEASUREMENTS

Qualitative Observations

Qualitative comparison of the normal and affected retinae for each group demonstrated differences in the cellular appearance of the RGC across conditions. The main effects of the nerve injury on RGC morphology were: irregularity of the cell surface and decreased RBPMS fluorescent stain intensity in both the cytoplasm and nucleus. These changes improved in the animals receiving eye treatment alone, and more so in those receiving the dual treatment strategy (Fig. 17).

Quantitative Observations

Retinal ganglion cell survival was determined by counting RBPMS-labeled RGCs in 36 regions of each retina, with equal samples obtained from all quadrants of the retina (Fig. 13).
In the 5 normal animals, the mean RGC cell count was 12,811± 914 for the left eye and 12,875± 1165 for the right eye. Based on an overall mean cell count of 12,843± 988, and our estimate that our sample region represents about 15% of the total area of the rat retina, this yields a total retinal ganglion cell estimate of approximately 85,620 for the normal rat eye, which is comparable to that of previous studies. [68-70]

Percent RGC survival under each treatment condition was defined as the number of cells in the experimental eye versus those in the contralateral control eye of the same animal. As there was no significant differences between the various retinal sampling zones across animals, the data were combined for all similar zones across the eyes for that condition.

In the normal animals, the mean difference in the percentage of RGCs in the left versus right eyes of the same animal was found to be 103.3±9% (Fig. 18). After the optic nerve injury and no treatment, ganglion cell survival was reduced to 57.5±9% in the affected eye compared with the normal control eye ($p < 0.05$). Treatment of the eye with 5 µl of BDNF at the time of the nerve injury resulted in a significant increase in ganglion cell survival (83.6±10%) relative to that measured in the non-treated eye ($p < 0.05$), a change of approximately 45% relative to the only crush group. Combining treatment of the eye at the time of injury with daily optogenetic stimulation of visual cortex over the 9 day survival period resulted in an additional (17%) increase in ganglion cell survival (97.9%) relative to treatment of the eye alone ($p < 0.05$).

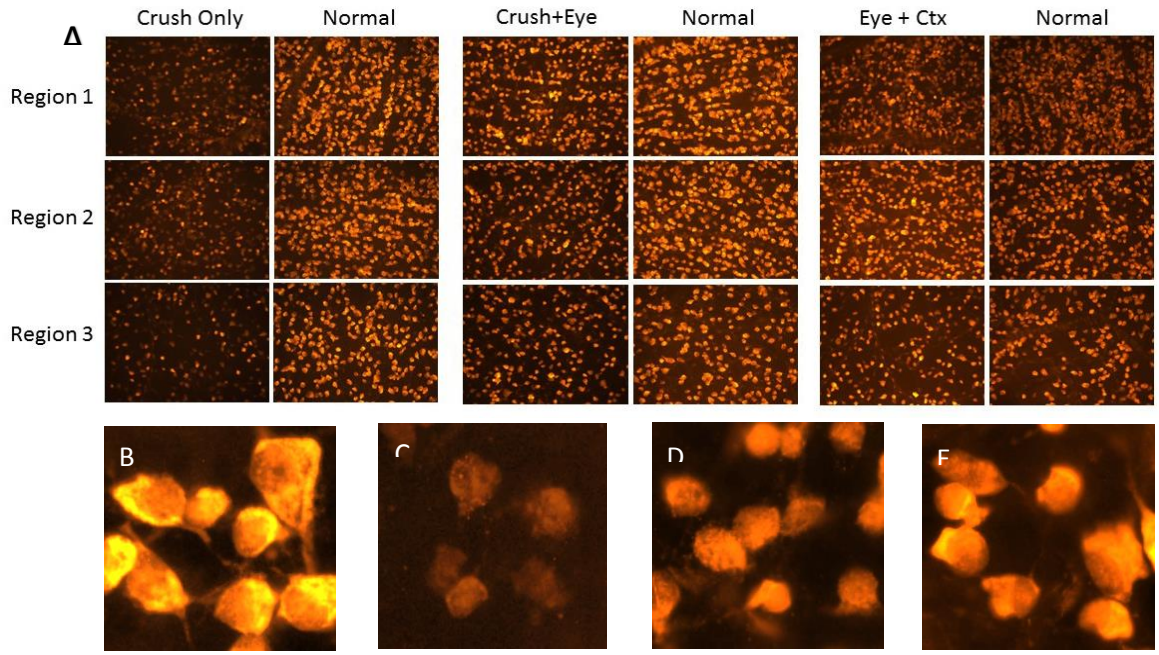

Figure 17: Retinal ganglion cell morphological features: A) Morphologic comparisons of the retinae from the experimental eyes with the normal fellow eyes in the three experimental groups. Ganglion cell images represent matched regions of the three zones of retina sampled. Bottom: Higher magnification images of matched regions of Zone 2 from B) normal eye, C) eye that received a mild, unilateral, nerve crush alone, D) eye treatment alone, and E) dual treatment. Image contrast was standardized B-D.

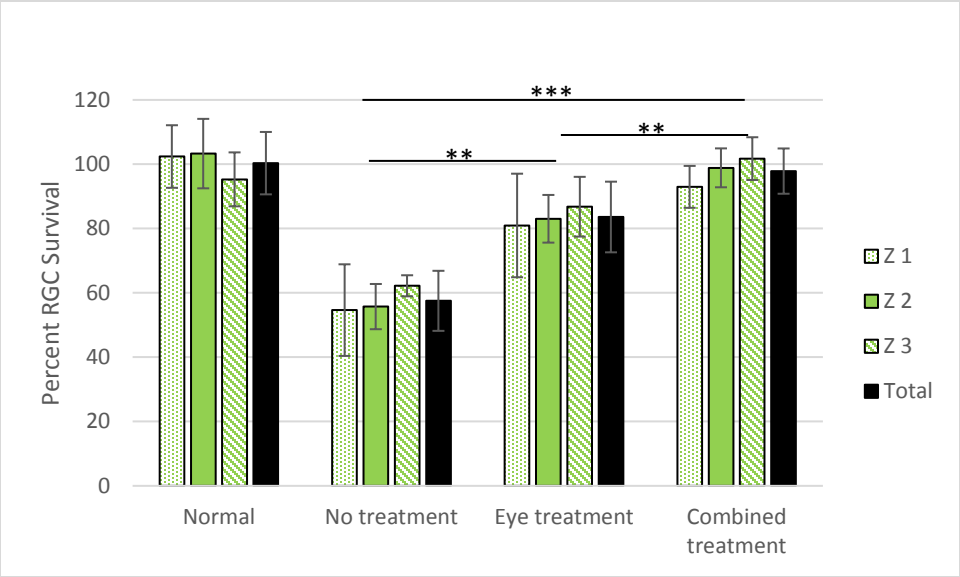

Figure 18: Comparison of percent ganglion cell survival in the retinas for animals receiving different treatment strategies and the 9 day survival period: There was a significant increase in ganglion cell survival following BDNF treatment to the eye alone ($p<0.05$) compared to no treatment. Animals that received both BDNF eye treatment combined with optogenetic stimulation of visual cortex showed a further significant ($p<0.05$) increase in cell survival compared to those that received the eye treatment alone, while there was no significant difference between the dual-treated animals and the normal control group. Z1 represents the retinal zone closest to the optic disc, Z2 is the mid-retinal zone, and Z3 is the peripheral zone. There was no difference between the three retinal zones with respect to loss of RGCs after the optic crush or following either follow treatment strategy.

OPTIC NERVE MEASUREMENTS

Cross sections of optic nerves were examined to compare optic nerve integrity (considering axons collapse; demyelination; and loss of the microfilament core, extent of preserving the characteristic shape of nerve fibers bundles and the amount of connective tissue between the nerve fiber bundles) of the untreated control eye optic nerves with those receiving either crush only, crush and eye treatment, or the dual treatment (Fig. 19). The masked analysis revealed that the optic nerves of all experimental groups were significantly different in appearance compared with the control group ($p < 0.05$). Although, the nerve cross sections exhibited a trend toward better scores in the dual treatment group (3.25) versus the crush only (3.85) and crush plus eye treatment group (3.6), these differences were not statistically significant ($p > 0.05$; Fig. 20).

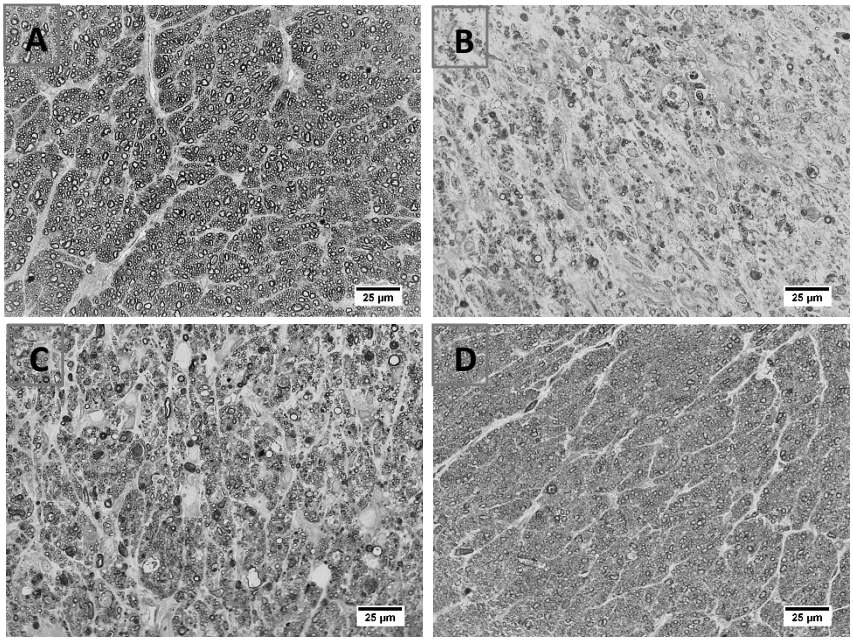

Figure 19: Optic nerve cross-sections showing the morphological characteristics of optic nerves from each of the four experimental groups: A) Normal optic nerve: score = 1, well defined nerve bundles and myelinated axons. B) Optic nerve from an animal that received a unilateral nerve crush and no treatment: score = 5, wide spread axonal degeneration, increased connective tissue around nerve fibers obscuring individual nerve bundles. C) Optic nerve from an animal that received BDNF treatment of the eye alone: score = 3, mixture of degenerating and well myelinated axons, nerve bundles still defined. D) Optic nerve from a dual treated animal: score = 2, although some degenerative profiles are visible, overall the axons and nerve bundles are comparable to normal.

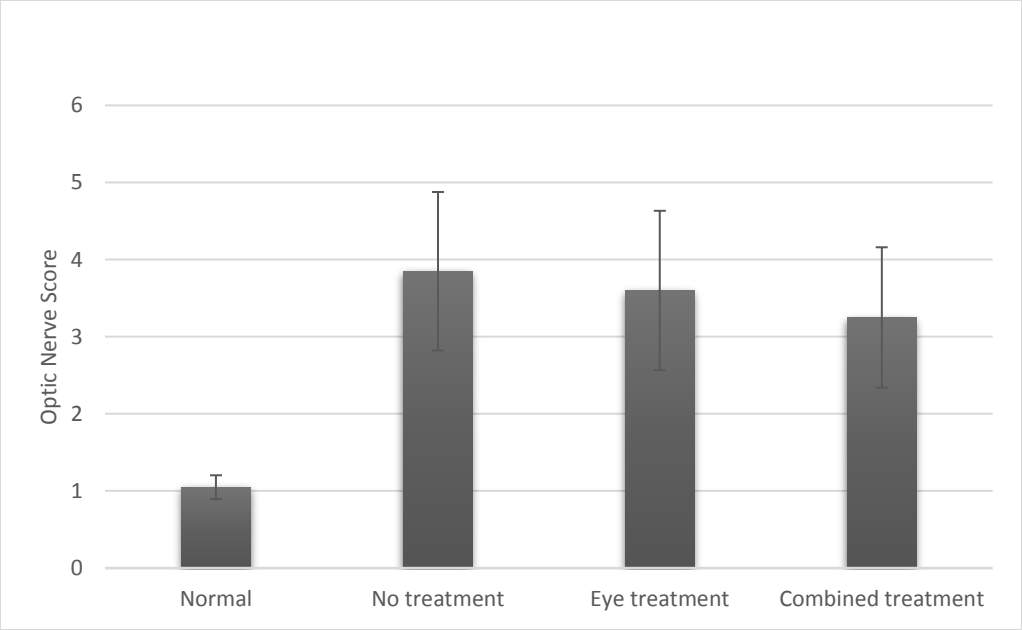

Figure 20: Comparison of optic nerve scores from animals receiving different treatment strategies and a 9 day survival period: (1 = normal; 5 = severely degenerated) There was a significant increase in the optic nerve scores following the nerve crush in all three groups compared to the normal animals ($p<0.05$). Although those animals that received eye treatment alone, or combined treatment of visual cortex and optogenetic stimulation showed improved nerve scores relative to the no treatment condition, the differences were not statistically significant ($p>0.05$)

ERG RECORDINGS

For baseline measurements, simultaneous ERG recordings were obtained from the right (normal) and left (affected) eyes of each animal prior to surgery. Figure 21 shows representative examples of ERG responses in each experimental group to flash stimuli of increasing intensity. The amplitudes of the pSTR increased with the increasing stimulus intensity. However, there was a significant bias in the pre-crush pSTR amplitudes, with the pSTR greater in the right versus left eye. This pre-recording bias appears to have resulted from a difference in the length of the corneal electrode leads – the significantly longer left eye lead may have provided more resistance, thus resulting in smaller amplitude responses from that eye. For comparison of ERG responses measured pre- and post-intervention between the same eye under each of the three experimental conditions, there was no significant difference in the mean response ratios between left and right eyes.

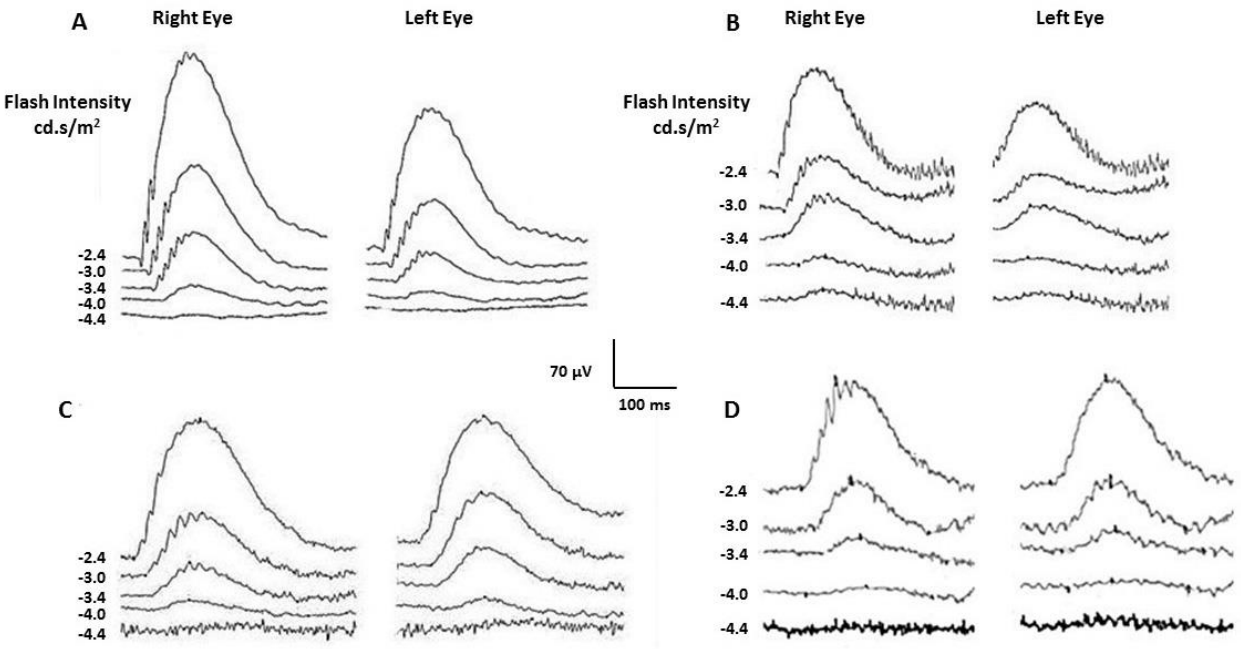

Figure 21: ERG recordings from the different experimental groups in response to flash stimuli of increasing intensity: Flash intensity is indicated at the left of each trace. A) ERG responses from a normal rat: note the increased amplitudes of the pSTR with increasing stimulus intensity. B-D) ERG responses following optic nerve crush only, crush with eye treatment alone, and crush with dual treatment following a 9 day survival period, respectively. ERG comparisons showed no significance differences between the four groups of animals.

DISCUSSION

The goal of this study was to examine the potential use of optogenetics as a novel neuroprotection strategy for preservation of retinal ganglion cell survival and function after optic nerve injury. By way of selective light stimulation, cells in visual cortex were induced to upregulate their expression of BDNF, and possibly other trophic materials. The rationale for this approach is that, in contrast to exogenous applications of trophic factors which have been shown to result in decreased drug efficacy due to drug-induced receptor down-regulation, stimulation of endogenous trophic expression might provide a more natural and stable level of support, thus resulting in enhanced neuroprotection.

Consistent with numerous previous studies, we too found that optogenetic stimulation of neurons transfected with the *ChR2* gene results in an increase in their level of c-fos expression, an early response protein indicative of increased neuronal activity. [72, 73] Earlier work also has demonstrated the relation between neuronal activity and BDNF expression. [90] Interestingly, the neuronal activity seen following stimulation of the transfected cells extended well beyond the confined area of viral transfection. A similar spread of enhanced c-fos expression in non-transfected neurons has been described by Covington, et al (2010). [74] The large number of local connections between cortical neurons could explain this pattern of signal propagation. [75, 76] The light stimulates the transfected cells directly, and then those neurons excite adjacent cells, which in turn excite the next population of cells, and so on. On the contralateral, non-stimulated side, the c-fos expression was restricted to site of the injection. This also was described by Lanshakov et al., (2017). [72] This enhancement of c-fos expression around the site of the AAV2 injection could

be attributed to immune cells that are activated as a result of an inflammatory response caused by the virus particles. [77, 78]

Interestingly, the widespread neuronal activity demonstrated by c-fos expression was not reflected in either the density or extent of BDNF expression, which was confined to the injected area. One explanation for this is that, since the cells within the injection site received the most intense stimulation, they correspondingly expressed levels of BDNF that were sufficient to be detected by immunostaining. Another possible explanation, based on the distinct shape of these cells, is that they represent a specific subtype of cells. They might be astrocytes, which have the ability to clear out excess levels of pro-BDNF secreted into the extracellular space during robust neuronal activity, or they may be activated stellate cells that produce BDNF but lack the ability to propagate the signal distally because they generally project only locally. [79, 80] However, the significant increase in retinal neuroprotection attained by the dual treatment also might be the result of contributions from neurotrophic factors other than BDNF. This possibility should be addressed in future studies.

In this study, we show that optogenetic stimulation of visual cortex combined with application of BDNF to the eye enhances retinal ganglion cell survival following mild optic nerve crush relative to no treatment or BDNF treatment of the eye alone. This is consistent with our previous studies in the cat where we found that treating the entire CVP by combining the intraocular injection with chronic infusion of BDNF to visual cortex produced the greatest level of neuroprotection. The thought behind this dual treatment approach is our hypothesis that injury to the optic nerve results in a decrease in retinal excitation of the visual thalamus and superior colliculi (SC), which in turn results in a decrease in the expression of trophic materials by

the neurons in these regions. This leads to a decrease in the normal levels of target-derived trophic materials required to maintain retinal ganglion cells, and thus failure of acute treatment of the eye alone to sustain RGC survival. Treatment at the level of visual cortex vs the visual thalamus or SC is beneficial due to the large reciprocal connections each have with the cortex. Because of this, stimulation of visual cortex may be beneficial for a couple different reasons. First, it results in increased production of trophic materials within visual cortex, which then are transported both anterogradely and retrogradely to the LGN and SC to support the retinal target neurons. Second, the increased electrical activity within visual cortex results in increased electrical activation of the thalamic or collicular neurons, inducing increased local endogenous trophic factor expression.

The optic nerve data suggest that the neuroprotective effects of BDNF were not restricted to retinal ganglion cells, but to their axons as well. However, perhaps due to the limited number of animals, the differences between the three experimental groups did not reach statistical significance. In addition, the optic nerve scores did not directly reflect our measurements of ganglion cell survival, suggesting that the effect of treatment at the level of the optic nerve may be delayed; for example, the dual treatment succeeded in preserving up to 97% of cells, while showing only a modest positive effect on optic nerve integrity. In previous work from our lab, optic nerve integrity improved after two weeks of injury and treatment in comparison to one week. [31] A similar pattern of discrepancy between cell survival and axon integrity, as well as the delayed effect of treatment on the optic nerve, was noted in other studies. [42, 48, 81]

In this study, the pSTR did not appear to be affected significantly by the optic nerve crush following the 9 day survival period. However, we noticed a significant bias with respect to the

pre-crush recordings from the two eyes of normal animals (see Methods). This bias in favor of the right eye appears to have resulted from a difference in the lengths of the ERG electrode leads. To minimize this bias effect which might compromise any real difference post-crush, we derived the left to right eye response ratios and compared these post- vs pre-treatment. The fact that we did not find a significant difference across experimental groups is difficult to reconcile with other studies that have shown a significant decrease of pSTR amplitudes after optic nerve injury. [82-88] This difference from other studies could have several possible explanations. First, these finding might be ascribed to the limited number of rats available to be tested functionally in this study (n=4) in comparison with most other studies (7-20). A key reason for favoring larger samples in ERG studies is the natural variability in the ERG, as described by Frishman et al., (2002). These variations were seen even when ERG recording sessions were repeated for the same animals. Potential causes of variability include the recording setup, level of anesthesia, extraneous electrical noise, or involuntary respiratory movements. [84] Second, the different optic nerve injury models and/or animal species also contribute to variations in ERG responses across studies, and this possibility can be applied to our results as well. [82-88] Third, the correlation between surviving retinal ganglion cell numbers and function as determined by full field flash ERG can be highly variable. [88] Two weeks post-optic nerve transection, Alarcón-Martínez et al., (2009) found that the pSTR amplitude decreased by 65% whereas, Fortune et al., (2003) reported a decrease of 90%, even though the RGC loss was greater (80%) in the first study than the second study (65%).[82, 83] In models of glaucoma, Mead et al., (2016) and Fortune et al., (2004) reported that elevation of IOP for 28-35 days resulted in a decrease of more than 70% in the amplitude of the pSTR [86,87] Nevertheless, these studies showed only a mild to moderate loss of RGCs. Thus, it is plausible

that we did not find a significant change in the pSTR amplitudes in our study due to the milder nerve crush and shorter survival period (9 days) used. Therefore, to reach a more firm conclusion with respect to optogenetic stimulation and RGC function in future studies, we recommend extending the survival period to 2-3 weeks with larger numbers of subjects (8-10) per group.

In addition to demonstrating that optogenetic stimulation of visual cortex is capable of enhancing endogenous production of BDNF, this study also suggests that such an approach might serve as an effective neuroprotective tool for preservation of retinal ganglion cells following injury to the optic nerve. To the best of our knowledge, this is the first study to demonstrate a significant preservation of RGCs following optogentic stimulation of visual cortex. These encouraging results also require future studies to investigate more thoroughly the effects of optogenetic stimulation at the molecular level, in particular its ability to induce endogenous expression of other trophic factors and to drive anti-apoptotic pathways. One also needs to better understand any potential negative effects of long-term stimulation. The promising results of this study also have implications for the application of this approach beyond the treatment of glaucoma to include optic neuropathies in general.

REFERENCES

REFERENCES

1. Quigley, H., & Broman, A. (2006). The number of people with glaucoma worldwide in 2010 and 2020. *British Journal of Ophthalmology, 90*(3), 262-267. doi:10.1136/bjo.2005.081224.

2. Tham, Y., Li, X., Wong, T., Quigley, H., Aung, T., & Cheng, C. (2014). Global prevalence of glaucoma and projections of glaucoma burden through 2040 A systematic review and meta-analysis. *Ophthalmology, 121*(11), 2081-2090. doi:10.1016/j.ophtha.2014.05.013.

3. Quigley, H., & Vitale, S. (1997). Models of open-angle glaucoma prevalence and incidence in the united states. *Investigative Ophthalmology & Visual Science, 38*(1), 83-91.

4. Agarwal, R., Gupta, S., Agarwal, P., Saxena, R., & Agrawal, S. (2009). Current concepts in the pathophysiology of glaucoma. *Indian Journal of Ophthalmology, 57*(4), 257-266. doi:10.4103/0301-4738.53049.

5. Davis, B. M., Crawley, L., Pahlitzsch, M., Javaid, F., & Cordeiro, M. F. (2016). Glaucoma: The retina and beyond. *Acta Neuropathologica, 132*(6), 807-826. doi:10.1007/s00401-016-1609-2.

6. Casson, R. J., Chidlow, G., Wood, J. P., Crowston, J. G., & Goldberg, I. (2012). Definition of glaucoma: Clinical and experimental concepts. *Clinical & Experimental Ophthalmology, 40*(4), 341-349. doi:10.1111/j.1442-9071.2012.02773.x

7. Mantravadi, A., & Vadhar, N. (2015) Glaucoma. *Primary Care, 42*(3), 437-437. doi:10.1016/j.pop.2015.05.008.

8. Gupta, D., & Chen, P. (2016). glaucoma. *American Family Physician, 93*(8), 668-674.

9. Weinreb, R. N., & Kheaw, P. T. (2004). Primary open-angle glaucoma. *The Lancet, 363*(9422), 1711-1720. doi:10.1016/S0140-6736(04)16257-0.

10. Weber, A. J. (2013). Autocrine and paracrine interactions and neuroprotection in glaucoma. *Cell and Tissue Research, 353*(2), 219-230. doi:10.1007/s00441-013-1556-3.

11. Burgoyne, C. F. (2010). Optic nerve: The glaucomatous optic nerve. (pp. 1-13). Berlin, Heidelberg: Springer Berlin Heidelberg. doi:10.1007/978-3-540-68240-0_1.

12. Koeppen, B. M., & Stanton, B. A. (2017). *Berne and levy physiology E-book* (7;7th; ed.). US: Elsevier.

13. Boron, W. F., & Boulpaep, E. L. (2012). *Medical physiology* Elsevier.

14. LeVere, T.E. (1978). The primary visual system of the rat: A primer of its anatomy. Psychobiology 6(2), 142-169.

15. Morgan, J. E. (2015). Pathogenesis of glaucomatous optic neuropathy. (Second ed., pp. 57-66) doi:10.1016/B978-0-7020-5193-7.00007-8.

16. Salinas-Navarro, M., Alarcon-Martinez, L., Valiente-Soriano, F., Jimenez-Lopez, M., Mayor-Torroglosa, S., Aviles-Trigueros, M., Vidal-Sanz, M. (2010). Ocular hypertension impairs optic nerve axonal transport leading to progressive retinal ganglion cell degeneration. *Experimental Eye Research, 90*(1), 168-183. doi:10.1016/j.exer.2009.10.003.

17. Lambiase, A., Aloe, L., Centofanti, M., Parisi, V., Mantelli, F., Colafrancesco, V., Levi-Montalcini, R. (2009). Experimental and clinical evidence of neuroprotection by nerve growth factor eye drops: Implications for glaucoma. *Proceedings of the National Academy of Sciences of the United States of America, 106*(32), 13469-13474. doi:10.1073/pnas.0906678106.

18. Fahy, E. T., Chrysostomou, V., & Crowston, J. G. (2015). Impaired axonal transport and glaucoma. *Current Eye Research,* 1-11. doi:10.3109/02713683.2015.1037924.

19. Lebrun-Julien, F., & Di Polo, A. (2008). Molecular and cell-based approaches for neuroprotection in glaucoma. *Optometry and Vision Science, 85*(6), 417-424. doi:10.1097/ OPX.0b013e31817841f7.

20. Adachi, N., Kohara, K., & Tsumoto, T. (2005). Difference in trafficking of brain-derived neurotrophic factor between axons and dendrites of cortical neurons, revealed by live-cell imaging. *BMC Neuroscience, 6*(1), 42-42. doi:10.1186/1471-2202-6-42.

21. Danesh-Meyer, H. V., & Levin, L. A. (2015). Glaucoma as a neurodegenerative disease. *Journal of Neuro-Ophthalmology, 35 Suppl 1*, S22-S28. doi:10.1097/WNO.0000000000000293.

22. Tezel, G., Kass, M. A., Kolker, A. E., Becker, B., & Wax, M. B. (1997). Plasma and aqueous humor endothelin levels in primary open-angle glaucoma. *Journal of Glaucoma, 6*(2), 83-89. doi:10.1097/00061198-199704000-00003.

23. Tan, O., Liu, G., Liang, L., Gao, S., Pechauer, A., Jia, Y., & Huang, D. (2015). En face doppler total retinal blood flow measurement with 70 kHz spectral optical coherence tomography. *Journal of Biomedical Optics, 20*(6), 066004. doi:10.1117/1.JBO.20.6.066004.

24. Kim, C., & Kim, T. (2009). Comparison of risk factors for bilateral and unilateral eye involvement in normal-tension glaucoma. *Investigative Ophthalmology & Visual Science, 50*(3), 1215-1220. doi:10.1167/iovs.08-1886.

25. Chang, E., & Goldberg, J. (2012). Glaucoma 2.0: Neuroprotection, neuroregeneration, neuroenhancement. *Ophthalmology, 119*(5), 979-986. doi:10.1016/j.ophtha.2011.11.003.

26. Squire, L. R. (2013;2012;). *Fundamental Neuroscience* (4th ed.). Amsterdam;Boston; Elsevier.

27. Rao, R. V., Bredesen, D. E., & Mehlen, P. (2006). Cell death in the nervous system. *Nature, 443*(7113), 796-802. doi:10.1038/nature05293.

28. Jindal, A. P. (2015, January 20). Medical Management for Primary Open Angle Glaucoma. Retrieved October 02, 2017, from http://eyewiki.org/Medical_Management_for_Primary_Open_Angle_Glaucoma#Mechanism_of_action.

29. Cheng, L., Sapieha, P., Kittlerova, P., Hauswirth, W. W., & Di Polo, A. (2002). TrkB gene transfer protects retinal ganglion cells from axotomy-induced death in vivo. *Journal of Neuroscience, 22*(10), 3977-3986.

30. Ma, Y., Hsieh, T., Forbes, M. E., Johnson, J. E., & Frost, D. O. (1998). BDNF injected into the superior colliculus reduces developmental retinal ganglion cell death. *Journal of Neuroscience, 18*(6), 2097-2107.

31. Weber, A. J., Viswanathan, S., Ramanathan, C., & Harman, C. D. (2010). Combined application of BDNF to the eye and brain enhances ganglion cell survival and function in the cat after optic nerve injury. *Investigative Ophthalmology & Visual Science, 51*(1), 327-334. doi:10.1167/iovs.09-3740.

32. Weber, A., & Harman, C. (2013). BDNF treatment and extended recovery from optic nerve trauma in the cat. *Investigative Ophthalmology & Visual Science, 54*(10), 6594-6604. doi:10.1167/iovs.13-12683.

33. Kimura, A., Namekata, K., Guo, X., Harada, C., & Harada, T. (2016). Neuroprotection, growth factors and BDNF-TrkB signalling in retinal degeneration. *International Journal of Molecular Sciences, 17*(9), 1584. doi:10.3390/ijms17091584.

34. Numakawa, T., Suzuki, S., Kumamaru, E., Adachi, N., Richards, M., & Kunugi, H. (2010). BDNF function and intracellular signaling in neurons. *Histology and Histopathology, 25*(2), 237-258.

35. Binder, D., & Scharfman, H. (2004). Brain-derived neurotrophic factor. *Growth Factors, 22*(3), 123-131. doi:10.1080/08977190410001723308.

36. Mey, J., & Thanos, S. (1993). Intravitreal injections of neurotrophic factors support the survival of axotomized retinal ganglion cells in adult rats in vivo. *Brain Research, 602*(2), 304-317. doi:10.1016/0006-8993(93)90695-J.

37. DiPolo, A. D., Aigner, L. J., Dunn, R. J., Bray, G. M., & Aguayo, A. J. (1998). Prolonged delivery of brain-derived neurotrophic factor by adenovirus-infected muller cells temporarily rescues injured retinal ganglion cells. *Proceedings of the National Academy of Sciences of the United States of America, 95*(7), 3978-3983. doi:10.1073/pnas.95.7.3978.

38. Klöcker, N., Kermer, P., Weishaupt, J. H., Labes, M., Ankerhold, R., & Bahr, M. (2000). Brain-derived neurotrophic factor-mediated neuroprotection of adult rat retinal ganglion cells in vivo does not exclusively depend on phosphatidyl-inositol-3'-Kinase/Protein kinase B signaling. *Journal of Neuroscience, 20*(18), 6962-6967.

39. Mansour-Robaey, S., Clarke, D. B., Wang, Y. -., Bray, G. M., & Aguayo, A. J. (1994). Effects of ocular injury and administration of brain-derived neurotrophic factor on survival and regrowth of axotomized retinal ganglion cells. *Proceedings of the National Academy of Sciences of the United States of America, 91*(5), 1632-1636. doi:10.1073/pnas.91.5.1632.

40. Nakazawa, T., Tamai, M., & Mori, N. (2002). Brain-derived neurotrophic factor prevents axotomized retinal ganglion cell death through MAPK and PI3K signaling pathways. *Investigative Ophthalmology & Visual Science, 43*(10), 3319-3326.

41. Peinado-Ramon, P., Salvador, M., Villegas-Perez, M., & Vidal-Sanz, M. (1996). Effects of axotomy and intraocular administration of NT-4, NT-3, and brain-derived neurotrophic factor on the survival of adult rat retinal ganglion cells. A quantitative in vivo study. *Investigative Ophthalmology & Visual Science, 37*(4), 489-500.

42. Weber, A., & Harman, C. (2008). BDNF preserves the dendritic morphology of alpha and beta ganglion cells in the cat retina after optic nerve injury. *Investigative Ophthalmology & Visual Science, 49*(6), 2456-2463. doi:10.1167/iovs.07-1325.

43. Chen, H., & Weber, A. J. (2004). Brain-derived neurotrophic factor reduces TrkB protein and mRNA in the normal retina and following optic nerve crush in adult rats. *Brain Research, 1011*(1), 99-106. doi:10.1016/j.brainres.2004.03.024.

44. Weber, A. J., Harman, C. D., & Viswanathan, S. (2008). Effects of optic nerve injury, glaucoma, and neuroprotection on the survival, structure, and function of ganglion cells in the mammalian retina. *The Journal of Physiology, 586*(18), 4393-4400. doi:10.1113/jphysiol.2008.156729.

45. Almasieh, M., Wilson, A. M., Morquette, B., Cueva Vargas, J. L., & Di Polo, A. (2012). The molecular basis of retinal ganglion cell death in glaucoma. *Progress in Retinal and Eye Research, 31*(2), 152-181. doi:10.1016/j.preteyeres.2011.11.002.

46. Aid, T., Kazantseva, A., Piirsoo, M., Palm, K., & Timmusk, T. (2007). Mouse and rat BDNF gene structure and expression revisited. *Journal of Neuroscience Research, 85*(3), 525-535. doi:10.1002/jnr.21139.

47. Greenberg, M. E., Xu, B., Lu, B., & Hempstead, B. L. (2009). New insights in the biology of BDNF synthesis and release: Implications in CNS function. *Journal of Neuroscience, 29*(41), 12764-12767. doi:10.1523/JNEUROSCI.3566-09.2009.

48. Harper, M., Grozdanic, S., Blits, B., Kuehn, M., Zamzow, D., Buss, J., Sakaguchi, D. (2011). Transplantation of BDNF-secreting mesenchymal stem cells provides neuroprotection in chronically hypertensive rat eyes. *Investigative Ophthalmology & Visual Science, 52*(7), 4506-4515. doi:10.1167/iovs.11-7346.

49. Gupta, N., & Yucel, Y. (2007). Should we treat the brain in glaucoma? *Canadian Journal of Ophthalmology- Journal Canadien d Ophtalmologie, 42*(3), 409-413. doi:10.3129/canjophthalmol.i07-051.

50. Gupta, N., Ang, L., de Tilly, L., Bidaisee, L., & Yucel, Y. (2006). Human glaucoma and neural degeneration in intracranial optic nerve, lateral geniculate nucleus, and visual cortex. *British Journal of Ophthalmology, 90*(6), 674-678. doi:10.1136/bjo.2005.086769.

51. Bareket-Keren, L., & Hanein, Y. (2014). Novel interfaces for light directed neuronal stimulation: Advances and challenges. *International Journal of Nanomedicine, 9*, 65-83. doi:10.2147/IJN.S51193.

52. Durand, R., Deisseroth, K., Zhang, F., Gradinaru, V., Airan, R. D., Adamantidis, A. R., & de Lecea, L. (2010). Optogenetic interrogation of neural circuits: Technology for probing mammalian brain structures. *Nature Protocols, 5*(3), 439-456. doi:10.1038/nprot.2009.226.

53. Deisseroth, K. (2011). optogenetics. *Nature Methods, 8*(1), 26-29. doi:10.1038/nmeth.f.324

54. Ernst, O., Lodowski, D., Elstner, M., Hegemann, P., Brown, L., & Kandori, H. (2014). Microbial and animal rhodopsins: Structures, functions, and molecular mechanisms. *Chemical Reviews, 114*(1), 126-163. doi:10.1021/cr4003769.

55. Parrilla-Reverter, G., Agudo, M., Sobrado-Calvo, P., Salinas-Navarro, M., Villegas-Pérez, M. P., & Vidal-Sanz, M. (2009). Effects of different neurotrophic factors on the survival of retinal ganglion cells after a complete intraorbital nerve crush injury: A quantitative in vivo study.Experimental Eye Research, 89(1), 32-41. doi:10.1016/j.exer.2009.02.015.

56. Sánchez-Migallón, M. C., Nadal-Nicolás, F. M., Jiménez-López, M., Sobrado-Calvo, P., Vidal-Sanz, M., & Agudo-Barriuso, M. (2011). Brain derived neurotrophic factor maintains Brn3a expression in axotomized rat retinal ganglion cells. Experimental Eye Research, 92(4), 260-267. doi:10.1016/j.exer.2011.02.001.

57. Pernet, V., & Di Polo, A. (2006). Synergistic action of brain-derived neurotrophic factor and lens injury promotes retinal ganglion cell survival, but leads to optic nerve dystrophy in vivo. Brain, 129(Pt 4), 1014-1026. doi:10.1093/brain/awl015.

58. Rodriguez, A. R., Sevilla Müller, L. P., & Brecha, N. C. (2014). The RNA binding protein RBPMS is a selective marker of ganglion cells in the mammalian retina. Journal of Comparative Neurology, 522(6), 1411-1443. doi:10.1002/cne.23521.

59. Morrison, J. C., Johnson, E. C., Cepurna, W., & Jia, L. (2005). Understanding mechanisms of pressure-induced optic nerve damage. Progress in Retinal and Eye Research, 24(2), 217-240. doi:10.1016/j.preteyeres.2004.08.003.

60. Weinreb, R. N., Aung, T., & Medeiros, F. A. (2014). The pathophysiology and treatment of glaucoma: A review. Jama, 311(18), 1901-1911. doi:10.1001/jama.2014.3192

61. J. Smith-Jeffries (2014). Resource: Visual Impairment and Blindness in the Senior Population. The Eighth Line. Retrieved from http://acao.ca.

62. Cunha, C., Brambilla, R., & Thomas, K. L. (2010). A simple role for BDNF in learning and memory? Frontiers in Molecular Neuroscience, 3, 1. doi:10.3389/neuro.02.001.2010.

63. Weber, A., Kaufman, P., & Hubbard, W. (1998). Morphology of single ganglion cells in the glaucomatous primate retina. Investigative Ophthalmology & Visual Science, 39(12), 2304.

64. Weber, A. J., Chen, H., Hubbard, W. C., & Kaufman, P. L. (2000). Experimental glaucoma and cell size, density, and number in the primate lateral geniculate nucleus. Investigative Ophthalmology & Visual Science, 41(6), 1370.

65. Weber, Arthur J., and Daryl Zelenak. (2001) Experimental Glaucoma in the Primate Induced by Latex Microspheres. Journal of Neuroscience Methods, vol. 111 (1), 39-48.

66. Gupta, N., Ang, L., Noël de Tilly, L., Bidaisee, L., & Yücel, Y. H. (2006). Human glaucoma and neural degeneration in intracranial optic nerve, lateral geniculate nucleus, and visual cortex. The British Journal of Ophthalmology, 90(6), 674-678. doi:10.1136/bjo.2005.086769.

67. Ocular pathology, 5th ed. (CD-ROM) (2002). Portland: Ringgold Inc.

68. Galindo-Romero, C., Jiménez-López, M., García-Ayuso, D., Salinas-Navarro, M., Nadal-Nicolás, F. M., Agudo-Barriuso, M., . . . Vidal-Sanz, M. (2013). Number and spatial distribution of intrinsically photosensitive retinal ganglion cells in the adult albino rat. Experimental Eye Research, 108, 84-93. doi:10.1016/j.exer.2012.12.010.

69. Salinas-Navarro, M., Mayor-Torroglosa, S., Jiménez-López, M., Avilés-Trigueros, M., Holmes, T. M., Lund, R. D., . . . Vidal-Sanz, M. (2009). A computerized analysis of the entire retinal ganglion cell population and its spatial distribution in adult rats. Vision Research, 49(1), 115-126. doi:10.1016/j.visres.2008.09.029.

70. García-Ayuso, D., Salinas-Navarro, M., Agudo, M., Cuenca, N., Pinilla, I., Vidal-Sanz, M., & Villegas-Pérez, M. P. (2010). Retinal ganglion cell numbers and delayed retinal ganglion cell death in the P23H rat retina. Experimental Eye Research, 91(6), 800-810. doi:10.1016/j.exer.2010.10.003.

71. Zhang, F., Deisseroth, K., Boyden, E. S., & Wang, L. (2006). Channelrhodopsin-2 and optical control of excitable cells. Nature Methods, 3(10), 785-792. doi:10.1038/nmeth936.

72. *Lanshak*ov, D. A., Drozd, U. S., & Dygalo, N. N. (2017). Optogenetic stimulation increases level of antiapoptotic protein bcl-xL in neurons. Biochemistry (Moscow), 82(3), 340-344. doi:10.1134/S0006297917030129.

73. Ramirez, S., Liu, X., MacDonald, C., Moffa, A., Zhou, J., Redondo, R., & Tonegawa, S. (2015). Activating positive memory engrams suppresses depression-like behaviour. Nature, 522(7556), 335-335. doi:10.1038/nature14514.

74. Covington, H., Lobo, M., Maze, I., Vialou, V., Hyman, J., Zaman, S., Nestler, E. (2010). Antidepressant effect of optogenetic stimulation of the medial prefrontal cortex. Journal of Neuroscience, 30(48), 16082-16090. doi:10.1523/JNEUROSCI.1731-10.2010.

75. Thanos, P., Robison, L., Nestler, E., Kim, R., Michaelides, M., Lobo, M., & Volkow, N. (2013). Mapping brain metabolic connectivity in awake rats with mu PET and optogenetic stimulation. Journal of Neuroscience, 33(15), 6343-6349. doi:10.1523/JNEUROSCI.4997-12.2013.

76. Leite, H. R., Oliveira-Lima, O. C. d., Pereira, G. S., Pereira, L. d. M., Oliveira, Vinícius Elias de Moura, Prado, M. A. M., Massensini, A. R. (2016). Vesicular acetylcholine transporter

knock down-mice are more susceptible to inflammation, c-fos expression and sickness behavior induced by lipopolysaccharide. Brain Behavior and Immunity, 57, 282-292. doi:10.1016/j.bbi.2016.05.005.

77. Kunitsyna, T. A., Ivashkina, O. I., Roshchina, M. A., Toropova, K. A., & Anokhin, K. V. (2016). Lentiviral transduction of neurons in adult brain: Evaluation of inflammatory response and cognitive effects in mice. Bulletin of Experimental Biology and Medicine, 161(2), 316-319. doi:10.1007/s10517-016-3404-4.

78. Aschauer, D., Kreuz, S., & Rumpel, S. (2013). Analysis of transduction efficiency, tropism and axonal transport of AAV serotypes 1, 2, 5, 6, 8 and 9 in the mouse brain. Plos One, 8(9), e76310. doi:10.1371/journal.pone.0076310.

79. Bergami, M., Santi, S., Formaggio, E., Cagnoli, C., Verderio, C., Blum, R., Canossa, M. (2008). Uptake and recycling of pro-BDNF for transmitter-induced secretion by cortical astrocytes. The Journal of Cell Biology, 183(2), 213-221. doi:10.1083/jcb.200806137.

80. Kepecs, A., & Fishell, G. (2014). Interneuron cell types are fit to function. Nature, 505(7483), 318-326. doi:10.1038/nature12983.

81. Ghaffarieh, A., & Levin, L. A. (2012). Optic nerve disease and axon pathophysiology. (pp. 1-17). SAN DIEGO: Elsevier Science & Technology. doi:10.1016/B978-0-12-398309-1.00002-0.

82. Bui, B. V., & Fortune, B. (2004). Ganglion cell contributions to the rat full-field electroretinogram: Ganglion cell responses in the rat ERG. The Journal of Physiology, 555(1), 153-173. doi:10.1113/jphysiol.2003.052738.

83. Alarcón-Martínez, L., de la Villa, P., Avilés-Trigueros, M., Blanco, R., Villegas-Pérez, M. P., & Vidal-Sanz, M. (2009). Short and long term axotomy-induced ERG changes in albino and pigmented rats. Molecular Vision, 15, 2373.

84. Saszik, S. M., Robson, J. G., & Frishman, L. J. (2002). The scotopic threshold response of the dark-adapted electroretinogram of the mouse. The Journal of Physiology, 543(3), 899-916. doi:10.1113/jphysiol.2002.019703.

85. Alarcón-Martínez, L., Avilés-Trigueros, M., Galindo-Romero, C., Valiente-Soriano, J., Agudo-Barriuso, M., Villa, P. d. l., Vidal-Sanz, M. (2010). ERG changes in albino and pigmented mice after optic nerve transection. Vision Research, 50(21), 2176-2187. doi:10.1016/j.visres.2010.08.014.

86. Mead, B., Hill, L. J., Blanch, R. J., Ward, K., Logan, A., Berry, M., . . . Scheven, B. A. (2015;2016;). Mesenchymal stromal cell–mediated neuroprotection and functional

preservation of retinal ganglion cells in a rodent model of glaucoma. Cytotherapy, 18(4), 487-496. doi:10.1016/j.jcyt.2015.12.002.

87. Fortune, B., Bui, B. V., Morrison, J. C., Johnson, E. C., Dong, J., Cepurna, W. O., Cioffi, G. A. (2004). Selective ganglion cell functional loss in rats with experimental glaucoma. Investigative Ophthalmology & Visual Science, 45(6), 1854. doi:10.1167/iovs.03-1411.

88. Mead, B., & Tomarev, S. (2016). Evaluating retinal ganglion cell loss and dysfunction. Experimental Eye Research, 151, 96-106. doi:10.1016/j.exer.2016.08.006.

89. Frishman, L. J., & Wang, M. H. (2011). Electroretinogram of human, monkey and mouse. (Eleventh ed., pp. 480-501) doi:10.1016/B978-0-323-05714-1.00024-8.

90. Glorioso, C., Sabatini, M., Unger, T., Hashimoto, T., Monteggia, L. M., Lewis, D. A., & Mirnics, K. (2006). Specificity and timing of neocortical transcriptome changes in response to BDNF gene ablation during embryogenesis or adulthood. Molecular Psychiatry, 11(7), 633-648. doi:10.1038/sj.mp.4001835.